Atomic force microscopy to elucidate how peptides disrupt membranes

Katharine Hammond,[1,2,3,*] *Maxim G Ryadnov*,[1,4,*] *and Bart W. Hoogenboom*[2,3,*]

[1]National Physical Laboratory, Hampton Road, Teddington, TW11 0LW, UK
[2]London Centre for Nanotechnology, University College London, London WC1H 0AH, UK
[3]Department of Physics & Astronomy, University College London, London WC1E 6BT, UK
[4]Department of Physics, King's College London, Strand Lane, London WC2R, UW

[*] kate.hammond@npl.co.uk, max.ryadnov@npl.co.uk, b.hoogenboom@ucl.ac.uk

Abstract

Atomic force microscopy is an increasingly attractive tool to study how peptides disrupt membranes. Often performed on reconstituted lipid bilayers, it provides access to time and length scales that allow dynamic investigations with nanometre resolution. Over the last decade, AFM studies have enabled visualisation of membrane disruption mechanisms by antimicrobial or host defence peptides, including peptides that target malignant cells and biofilms. Moreover, the emergence of high-speed modalities of the technique broadens the scope of investigations to antimicrobial kinetics as well as the imaging of peptide action on live cells in real time. This review describes how methodological advances in AFM facilitate new insights into membrane disruption mechanisms.

Key words

Atomic force microscopy, antimicrobial peptides, membrane disruption, supported lipid bilayers, phospholipid membranes, high resolution imaging

1. Introduction

1.1. Atomic force microscopy: basics and membrane imaging

1.1.1. Principles of atomic force microscopy

Since its invention in 1986 and subsequent adaptation for imaging in liquid, AFM has made significant contributions to our understanding of biological systems.[1] Samples, from single molecules to whole cells, can be visualised under near-native conditions, at (sub) nanometre resolution over timescales of seconds to hours. The basic principle of AFM is that a nanometre sharp tip mounted on a flexible cantilever is scanned across a surface, and the distance-dependent interaction forces between the tip and the sample are used to detect the proximity of the surface and to build an image as the tip follows the surface contours (Fig 1A).

In its simplest mode of operation, contact mode, the tip remains in contact with the surface during imaging. A feedback system continuously adjusts the *Z* position of the sample (or cantilever) to maintain a set applied force. Precise tip-sample adjustments are achieved by a piezoelectric motor and are used to create a topographical image of the sample. Many AFM imaging modes have been developed, and most operate on this principle of adjusting the tip-sample distance to nullify deviations from a constant average applied force.

For biological systems, dynamic mode is typically used. The cantilever is oscillated near to its resonance frequency and only comes into contact with the sample at the bottom of each oscillation, removing the high lateral forces present in contact mode. Dynamic mode AFM is the fastest imaging mode available and has enabled tracking of biomolecular processes at high temporal resolution.[2] Ongoing developments to cantilevers, controllers, piezoelectric scanners and detection systems are increasing the temporal resolution that can be achieved.[3]

The versatility of AFM cannot be understated. In force-distance (FD) curve imaging modes, mechanical properties can be extracted from each force-curve, and the stiffness, adhesion, deformation and dissipation of the sample can be quantified.[4] Modifications to the AFM tip can enable probing of electric and magnetic properties, or targeting of specific molecules such as cell surface receptors.[5] And, as well as sensing the surface, AFM can be used as a nanotool to manipulate the sample [1] even inducing cell division.[6] In this review, we focus on the application of AFM to elucidating mechanisms of lipid membrane disruption.

1.1.2. Imaging phospholipid membranes

Cell membranes consist of a fluid lipid bilayer that is packed with integral and peripheral proteins.[7] The bilayer has multiple roles, such as to regulate the passage of nutrients and ions, to support osmosis, to control molecular transport and to facilitate key events of normal cell physiology such as endocytosis. However, lipid bilayers are challenging to study. At only a few nanometres thick, they are unstable in air and highly dynamic. AFM has had considerable success in investigating the properties of fluid lipid assemblies. The formation, dynamics and lateral organisation of both bilayer and monolayer assemblies have been extensively characterised (see, e.g., ref [8–12]). Following this success, interest has grown in applying the same techniques to study mechanisms of induced membrane disruption.

To be compatible with AFM analysis, lipid bilayers are prepared on an underlying solid support. This is typically done using Langmuir-Blodgett (LB) [13] or vesicle deposition methods.[14, 15] The LB method uses sequential deposition of single lipid monolayers and is used for the preparation of asymmetric lipid bilayers or lipid monolayers. The vesicle fusion method relies on the spontaneous adsorption and rupture of lipid vesicles onto a hydrophilic solid support and is used to prepare supported lipid bilayers (SLBs). The process depends on the electrostatic interactions between the

vesicles and the solid support; optimal bilayer formation is controlled by adjusting the pH and the ionic strength of solution.[10] For AFM studies the underlying substrate is typically mica as it can be cleaved to produce an atomically flat surface. SLBs prepared on mica are flat to within a few angstroms and are compatible with high resolution imaging (Fig 1B).[16] Other hydrophilic surfaces may be preferred if correlative experiments are being performed, e.g., glass (for simultaneous optical or fluorescence), silica (for comparison to QCM-D) or functionalised gold (for simultaneous electrical measurements).

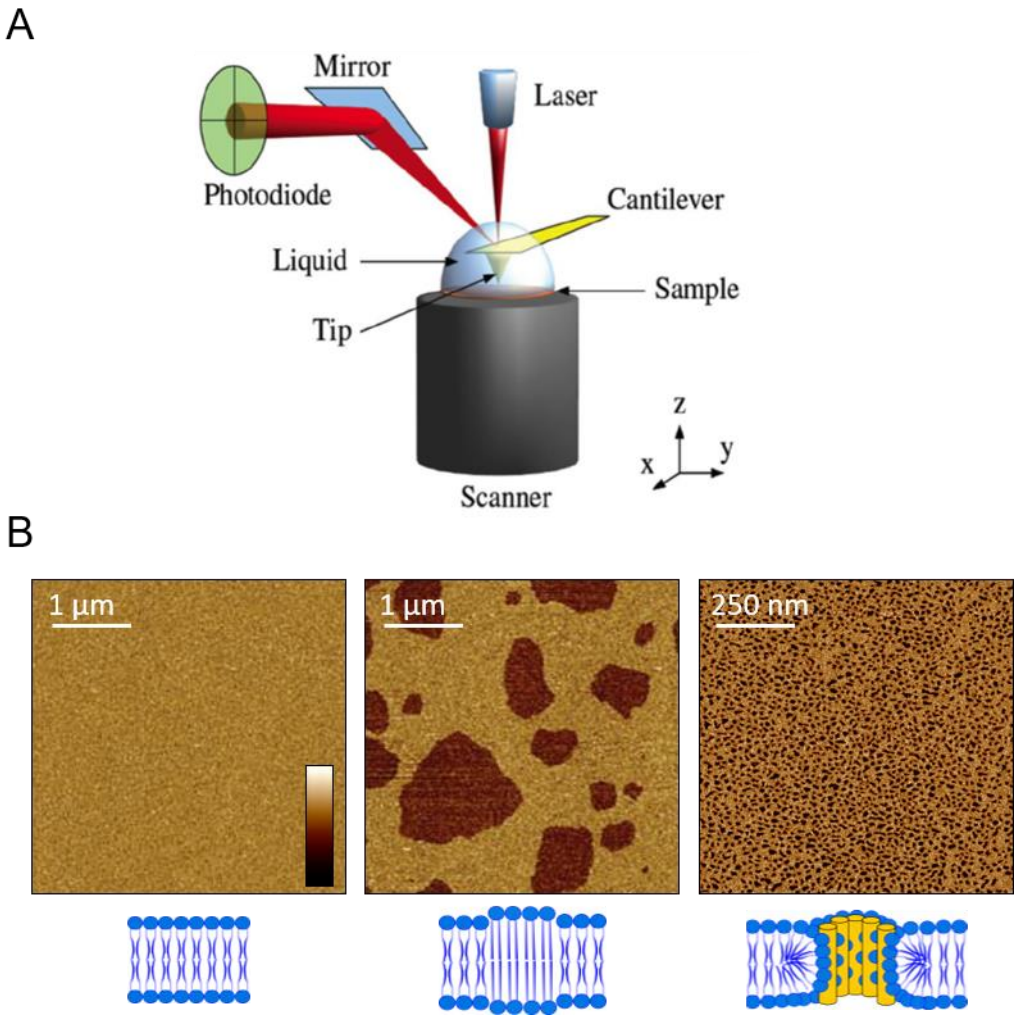

Figure 1. (A) Schematic showing the operation of AFM in liquid, reproduced from ref [17], permission pending. (B) AFM observation of SLBs. Left, topography of a single phase SLB. The surface is featureless and flat to within < 1 nm. Middle, topography of a phase separated SLB. L_d domains (darker) are here 1 nm lower/thinner than L_o domains (brighter). Right, topography of an SLB after addition of a pore-forming peptide, magainin 2. Pores with a diameter of 10 – 20 nm (black) can be observed across the surface. Colour (height) scale bar is 3 nm in all images. Left and middle images are reproduced from ref [18], licensed under CC BY 4.0, right image is original data.

Biological membranes are complex systems which can include hundreds of different lipid species, sugars and proteins. Phospholipids are the most abundant class of lipid and are the main component of SLBs prepared as biological membrane mimics.[19] Different phospholipids have different chain lengths, saturation, charge and curvature, and the specific lipids used will dictate the thickness, surface charge, and packing of the resulting SLB. Lipid composition can therefore be tuned to better mimic the properties of the target membrane.

A consideration when preparing an SLB is the desired fluidity. Lipid bilayers can form as fluid liquid disordered phases (L_d) or more solid gel state phases (S_o) depending on the temperature and the composition of the lipids, with every lipid having a unique melting temperature (T_m) below which they constitute membranes in a solid gel state and above which they preferentially adopt liquid phases. Biological membranes exist as liquid phases and with the exception of very specific examples (see, e.g. [20]) the gel-state phase is not physiologically observed.

In eukaryotic cells, fluidity across the membrane is not homogenous. Cholesterol can interact preferentially with lipids such as sphingomyelin, condensing into so-called liquid ordered phase (L_o) domains, which show increased packing density and lateral order of acyl chains whilst retaining fluidity.[21] The eukaryotic plasma membrane is rich in cholesterol and recent analysis of the plasma membrane of live HeLa cells measured 76% L_o regions to 24% L_d regions.[22] To mimic this, mixed L_o + L_d SLBs can be prepared by using lipid mixtures with different T_m values and incorporating hydrophobic intercalating molecules to induce localised lipid order.[23] Domains of differing fluidity show reduced or increased thickness and can be distinguished by AFM (Fig 1B). This allows phase-dependent processes to be resolved.[18]

Bacterial membranes have typically been considered single fluid phases but increasing evidence indicates they may also contain domains.[24, 25] Regions of higher fluidity may be driven by clustering of lipid II molecules,[26] and regions of lower fluidity may be induced by the presence of hopanoids, proposed to act as a functional equivalent to cholesterol and detected in some bacterial strains.[27] Furthermore, domain formation can be induced by a number of other factors such as lipid curvature preference, protein interactions and the underlying cytoskeleton[28] and heterogenous segregation of both PE and CL phospholipids has been observed in bacterial cells.[24, 29] As our understanding of the bacterial membrane organisation increases, adjustments to a single fluid phase SLBs as a model bacterial membrane may be required.

The spatial resolution limit of AFM imaging of SLBs is largely defined by experimental conditions rather than by instrumentation. When lipid assemblies are prepared below the fluid-to-gel transition temperature, the lateral diffusion of lipids within the assembly is slow (with diffusion coefficient D ~10^{-3} μm^2 s^{-1}).[19] AFM imaging of such assemblies has resolved individual lipid head groups with sub-nanometre lateral resolution.[30] However in fluid bilayers the diffusion of each lipid is orders of

magnitude faster than even the highest-speed AFM can currently acquire an image (D ~2 $\mu m^2 s^{-1}$), so a temporal average of the bilayer is visualised and individual lipids are not resolved.[19]

Membrane disrupting agents change the local organisation of lipid bilayers and this change can be directly visualised by AFM (e.g. poration, Fig 1B). Host defence peptides are now an object of choice for AFM investigations due to their ability to target and physically alter phospholipid bilayers.

1.2. Host defence peptides

Host defence or antimicrobial peptides (AMPs) are ubiquitous for all forms of life. The peptides target cellular membranes and can act as killing factors against microbial and malignant cells alike.[31, 32]. Structure-activity relationships for the peptides are relatively well understood and traditional methods such as neutron diffraction[33–36] and nuclear magnetic resonance spectroscopy[37–40] have provided important insights into the mode of action of these molecules.

Peptide-induced membrane disruption has also been visualised on bacterial cells by electron microscopy.[41, 42] However, before the advent of AFM much information pertaining to membrane-disruption mechanisms remained untapped. Over the last decade, its rapidly evolving capability has made significant contributions to the elucidation of poration mechanisms for a range of host defence peptides and activities, from antimicrobial to anticancer. Principally, owing to its nanoscale accuracy, AFM imaging has enabled fundamentally new insights into the architecture, abundance and dynamics of pore formation, which nowadays can be accessed with the spatiotemporal resolution unmatched by other methods. In this review, we discuss such contributions, emphasising the diversity of antimicrobial mechanisms and their dependence on experimental conditions, and provide an outlook on future capability developments and anticipated findings improving our understanding of membrane disruption mechanisms.

1.2.1. Structure and mechanism

Host defence peptides disrupt membranes by folding in the phospholipid bilayers as amphipathic secondary structures, α-helices or β-strands. These structures segregate their amino-acid residues into polar and hydrophobic faces, which bind to lipid headgroups and aliphatic chains, respectively. Upon insertion, the peptides assemble into peptide-lipid complexes, which disrupt the membrane by porating, thinning or corrugating the bilayer.[43] The membrane contains different lipid types at different combinations in different organisms. The lipid composition influences the charge, thickness, curvature and fluidity of the membrane, which can favour or resist interactions with the peptides.

In bacteria, antimicrobial peptides, which are typically cationic, target anionic lipids such as cardiolipin (CL) and phosphatidylglycerol (PG). This is the main basis for their selectivity towards microbial membranes over mammalian membranes.[44] Although the mammalian membrane also contains anionic phospholipids such as phosphatidylserine (PS), these are typically located in the

inner leaflet. The outer leaflet of mammalian membranes is rich in zwitterionic phosphatidylcholine (PC) and sphingomyelin (SM) lipids, which makes the membrane zwitterionic.[19] Malignant transformations can lead to increased exposure of anionic phospholipids in the outer leaflet, and, along with other changes in lipid composition, increase surface charge increasing cell susceptibility to the attack of host defence peptides.[45, 46] For example, the AMP temporin-1CEa, which shows high affinity for PS phospholipids, was shown to exhibit potent activity against cancer cells, which correlated with the overexpression of PS.[47]

Despite coevolution with bacteria over millions of years, high-level resistance to antimicrobial peptides has not emerged, which is the main reason for antimicrobial peptides to be considered as next-generation antibiotics.[48] Multiple resistance mechanisms against AMPs have been characterised including the secretion of proteins or lipids to sequester the peptides, peptide antagonists that co-fold with antimicrobial peptides and neutralise them,[49] cell-surface fortification that resist peptide binding and membrane thickening that reduce disruption effects.[48, 50] However, resistance conferred is moderate and often non-specific.[48] This leads to slow increases in MIC rather than the highly effective resistance observed for conventional antibiotics, which can quickly spread through horizontal gene transfer of dedicated resistant genes.[51] Daptomycin, an AMP in therapeutic use since 2003, provides clinical evidence for this with bacterial resistance observed at both low frequency and low potency.[52] Therapeutic interest in AMPs is furthered by their ability to penetrate difficult-to-treat non-planktonic microbial populations such as bacterial and fungal biofilms.[53, 54] Antiviral potential has also been demonstrated: the membrane activity of antimicrobial peptides extends to their ability to bind to enveloped viruses disrupting their envelop membranes,[55–58] or preventing their uncoating.[59, 60]

To guide the development of therapeutic applications for host defence peptides, naturally occurring or synthetic, it is crucial to understand how the peptides target and affect microbial membranes.[31] Given this importance, the activity of the peptides has been extensively reviewed (see, e.g., ref. [61]), considering three main models of membrane disruption by the peptides: the barrel-stave model, the carpet model, and the toroidal pore model.

In the barrel-stave model, peptide molecules insert into the membrane and stack side-by-side to form a transmembrane pore lined entirely by peptide (Fig 2A).[62] In the toroidal pore model, peptides complex with phospholipids by pulling their headgroups inwards to line the inner pore wall. The resulting pores are lined with both peptides and lipids (Fig 2B).[63, 64] In the carpet model, AMPs corrugate the surface of the membrane without inserting.[65] Above a threshold concentration, the carpet model can lead to membrane collapse with peptide-lipid micellization (Fig 2C). Other mechanisms of pore formation have also been proposed, including domain formation (Fig 2D), localised thinning (Fig 2F, 2G), and non-lytic depolarisation.[43]

The permeabilising effect of host defence peptides is commonly assessed using fluorescence leakage assays,[66–68] while their conformational preferences are determined using circular dichroism (CD) spectroscopy methods, which can also probe their alignment relative to the bilayer.[69, 70] NMR spectra help elucidate the structure of the peptides,[37] which are often complemented with molecular dynamics (MD) simulations to provide atomic-level structural descriptions.[71–75] Complementing such studies, AFM measurements fill a unique niche by probing membrane disruption effects in aqueous solutions at sub-nanometre spatial resolution,[1] with the added benefit of visualising changes in the membrane in real time.

2. Visualisation of AMP-membrane disruption

Here, we describe the use of AFM for visualisation of membrane disruption mechanisms by antimicrobial peptides and their derivatives. We do not focus on assigning particular mechanisms to specific peptides or lipid compositions, but rather on the variety of effects that have been observed, since the action of host defence peptides is normally conformation-dependent and is subject to environmental conditions.[50, 61]

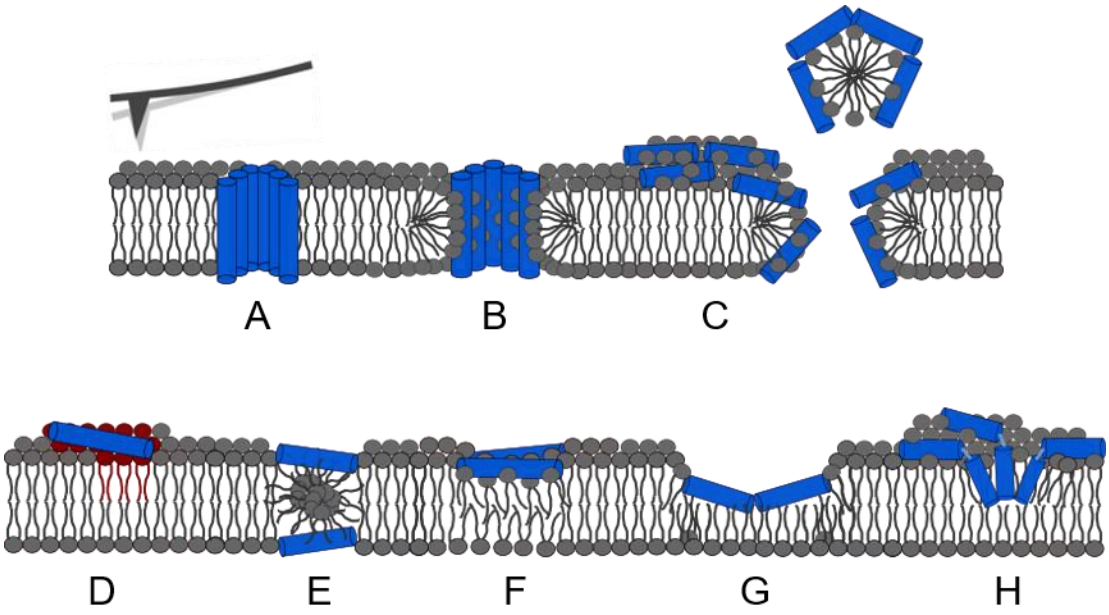

Figure 2. Peptide-induced membrane disruption mechanisms that can be identified by AFM. (A) barrel-stave poration; (B) toroidal pores; (C) carpet disruption leading to micellization; (D) phospholipid clustering; (E) induction of non-lamellar phase; (F) bilayer thinning; (G) monolayer removal; and (H) nanoscale pits.

2.1. Membrane disruption models: barrel-stave, toroidal pore and carpet models

AFM has been able to resolve membrane disruptions that are consistent with all three models, barrel stave, carpet and toroidal poration (Fig 2A-C).[76–80] For example, imaged at a sub-nanometre

resolution, alamethicin was found to create pores with a nominal diameter of 1.8 nm, smaller than a typical radius of AFM tips, and consistent with the barrel-stave pore model (Fig 3A).[76, 77] Cecropin B (CecB) showed overall membrane roughening by peptide consistent with the carpet model and for ChoC (a chopped analogue of Cecropin B), AFM images revealed larger pores, likely to be consistent with the toroidal pore model because of irregularities in their sizes and shapes (Fig 3B).[78]

2.2. Membrane thinning

Membrane thinning is a common result of antimicrobial attack, and was first measured by lamellar X-ray diffraction – the degree of thinning was found to be proportional to peptide concentration.[81, 82] Based on experimental findings, two models were proposed: (i) peptide binding results in discrete patches of thinned membranes of fixed depth, which grow laterally as more peptide is added; and (ii) peptide addition results in uniform thinning across the membrane, which gets progressively deeper as more peptide is added. X-ray diffraction is an averaging technique and cannot distinguish between these two models. In contrast, AFM is able to deconvolute these two thinning scenarios and shed light on mechanistic variations of membrane thinning.[83]

2.2.1. Micron-sized domains

Large domains with depths not exceeding 2 nm can also be observed in the membrane as a result of peptide treatment. These domains grow laterally with increasing peptide concentration. As for other thinned membranes, their depth remains constant. AFM helped visualise this effect for a variety of antimicrobial peptides including pexiganan (an analogue of magainin),[83] ChoM (an analogue of cecropin B, Fig 3B),[78] α-synuclein[84] and tilamin (a synthetic antimicrobial peptide).[85] However, the exact nature of such domains remains unclear. Proposed models include peptide-enriched domains where peptide binding causes acyl lipid chains to splay and thin (Fig 2F), or lipid-monolayer domains where the upper lipid leaflet becomes displaced by peptide (Fig 2G). The measured domain depths differ across studies, from 0.8 to 2 nm.

2.2.2. Uniform thinning

When SLBs are prepared in patches rather than as a continuous membrane, AFM can measure the height difference between the bilayer surface and the underlying solid support before and after peptide addition. Homogenous expansion and thinning of the membrane patch was observed by AFM, with up to a 25% reduction in height.[86, 87]

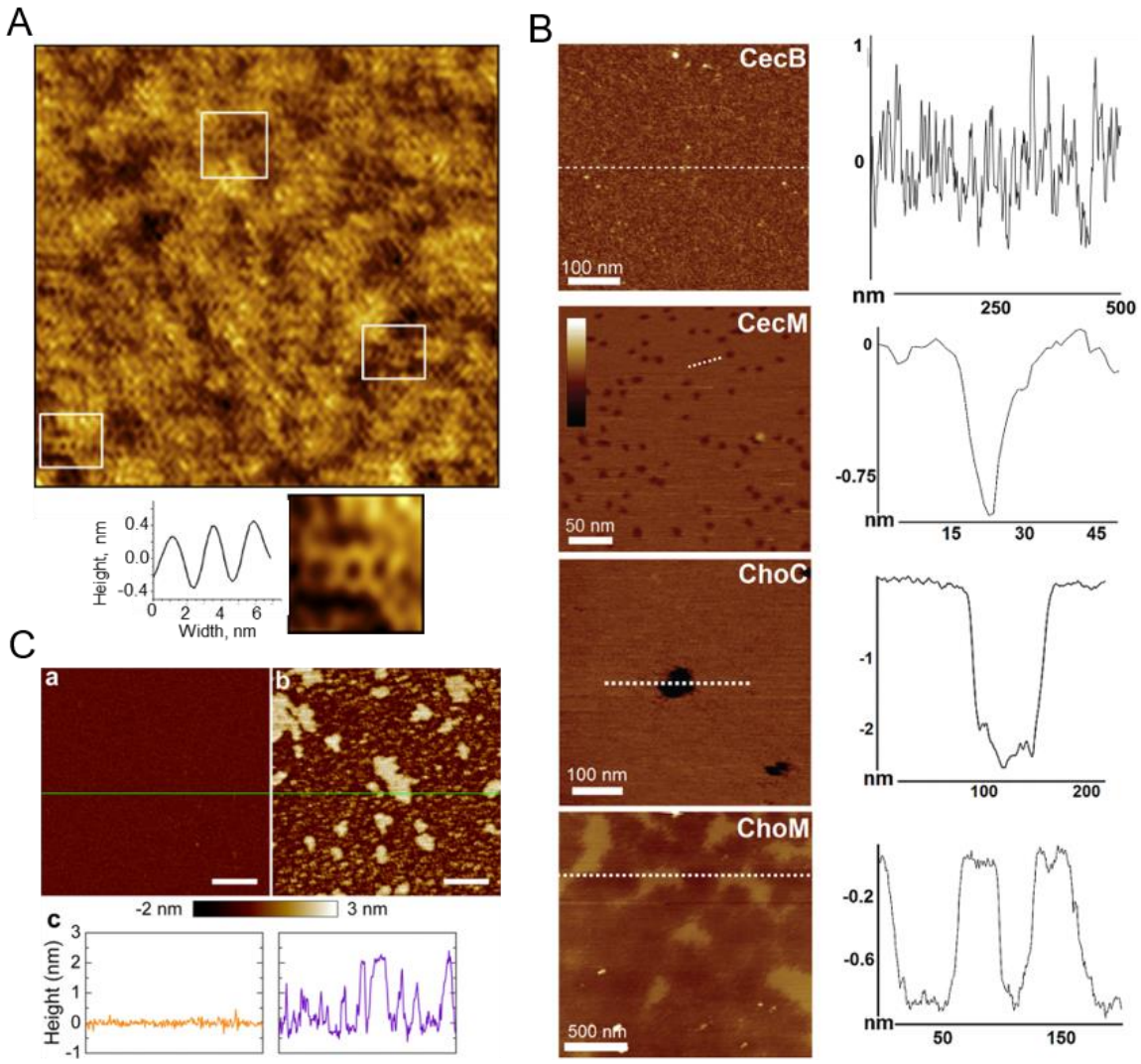

Figure 3. AFM observation of AMP disruption on supported lipid bilayers (SLBs). (A) AFM topography image of an alamethicin-treated SLB formed on a gold (111) electrode functionalised with a 1-thio-β-D-glucose (β-Tg) self-assembled monolayer (size 100 nm x 100 nm). A line profile of pores and a magnified area are shown underneath. Reproduced from ref [77], with permission from Elsevier. (B) Alterations in cecropin AMPs lead to different poration mechanisms (from top to bottom: carpet model, nanoscale pits, toroidal pore model and membrane thinning). AFM topography images (left) and cross-sections along the highlighted lines (right). Colour scale 6 nm. Reproduced from ref [78], licensed under CC BY 4.0. (C) Topography images before (a) and after (b) adding colistin to a mixed POPC/LPS bilayer. Colistin causes 2 nm high clusters. Cross sections are given in (c). Scale bars 200 nm. Reproduced from ref [88], licensed under ACS AuthorChoice, with permission from ACS.

2.2.3. Nanoscale pits

Recently, discrete localised pits were detected with sizes of up to 15 nm in diameter and less than 1 nm in depth indicative of that poration was limited to the upper leaflet the bilayer (Fig 3B, CecM).[78,

89] The observed wedge-like shape of these pits is consistent with peptides remaining anchored to the bilayer interface, with hydrophobic residues likely to obliquely insert into the acyl chains (and the pits appear too wide to attribute this shape to an AFM tip artefact) (Fig 2H).

2.2.4. Diffused thinning

Regions of diffused membrane thinning that move laterally across the surface were demonstrated for a melittin derivative, MelP5.[90] The peptide causes the formation of highly localised voids in the bilayer, but also non-localised thinning patches, which appear 0.3 nm deep into the membrane and tens of nanometres wide. In contrast to the large domains, which are micron-sized, these regions appear shallower, less defined and may represent heterogeneous aggregation of peptide at the bilayer surface.

2.3. Phospholipid clustering

AFM was shown to resolve lipid clustering effects in multi-compositional bilayers (Fig 2D). For example, in mixed POPC/LPS bilayers, colistin re-arranges the lateral organisation by forming LPS/colistin rich domains, which are 2 nm higher than the surrounding zwitterionic lipids (Fig 3C).[88] In a study combining AFM and leakage assays, evidence was obtained for lipid clustering leading to increased permeation. Specifically, AFM images showed that the number of clusters positively correlated with LPS and colistin concentrations, and so did membrane permeabilisation as gauged by leakage assays. By AFM, no clusters were formed with Mg^{2+} ions present (as Mg^{2+} binds strongly to LPS and may prevent colistin-LPS interactions), with no leakage observed in the presence of Mg^{2+} either.

In another recent example, P(G)KY20 was found to induce domain formation in POPC:PG (8:2) SLBs, with a height difference between domains measuring to < 1 nm.[91] Differential scanning calorimetry (DSC) showed this peptide segregated PC and PG lipids, where the single phase transition of DPPC:POPG (8:2) liposomes split into two distinct phase transitions, lower and higher, which indicated transitions to POPG and DPPC rich domains, respectively. The separation is likely driven by electrostatic interactions between cationic peptide molecules and anionic PG lipids. Based on these results, it was proposed that the higher domains observed by AFM represented clusters of POPG lipids, as the concentrations of peptide bound to the surface increased. However, the lower domains could represent POPG/peptide rich clusters, where peptide binding caused localised thinning. Whilst AFM can readily visualised differences in peptide preference for different lipid phases, it can therefore be difficult to interpret without additional experiments. Lipid segregation as well as localised membrane thinning and membrane thickening can all produce similar topographical effects.

In any case, the formation of domains in the membrane compromises the membrane integrity. The domain edges introduce discontinuities in the membrane where solutes may more easily pass through.

Furthermore, the segregation of lipids restricts their lateral mobility, reducing the ability of the bilayer to repair.[92]

2.4. Induction of non-lamellar phase

Antimicrobial peptides can alter the lipid packing of the bilayer. In PE-containing bilayers, the peptides can induce membrane rearrangement by releasing locally stored curvature stress.[93] PE has an intrinsic negative curvature and while it can form thermodynamically stable bilayers, it is prone to forming inverted hexagonal phases (Fig 2E).[94] The induction of non-lamellar phases in PE/PC and PE/PG bilayers was observed by AFM .[95] Stratifications with a depth of 0.3 - 1 nm appear in the membrane; both this decrease in thickness and the elongated nature of the stratifications are consistent with an inverted hexagonal phase.

AFM showed that such non-lamellar phases can be induced in SLBs that only contain bilayer-forming PC lipids. Henderson et al visualised the transformation of a DMPC membrane patch from a lamellar phase bilayer into worm-like micelles (Fig 4A, 0.7 μM AMP).[86] The height of the membrane was significantly reduced, from 3.7 nm in the unperturbed bilayer to 2.7 nm after peptide addition, incompatible with a lamellar phase DMPC bilayer. Similar transformations were observed for a DMPC/PG lipid patch by Hall et al.[87]

2.5. Lipid extraction and re-fusion

AMPs can also act like detergents, removing lipid from the bilayer through solubilisation.[87, 96] Furthermore, AFM studies show that extracted lipids can re-fuse to the bilayer surface, forming additional secondary bilayers as well as bound aggregates, and that re-fusion is promoted by anionic lipids, an acidic pH and cholesterol.[97] These findings are in agreement with previous studies demonstrating fusogenic properties of host defence peptides, and of parallel fusion and disruption mechanisms.[98, 99]

2.6. AMPs as line-active agents

AFM proves to make significant contributions into a better understanding of how peptides can stabilise, create and expand membrane edges by lowering the line tension.[86] For instance, lipid bilayer patches in contrast to continuous bilayers spontaneously form compact, round areas, thus minimising the length of the patch boundaries. This is due to the line tension that arises from the energy cost of re-arranging lipids at the boundary edges. The effect observed for 13 different antimicrobial peptides,[86] including unfolded and folded as α-helices, β-sheets and α-β structures having cationic, anionic and neutral net charges. All but one of the peptides caused significant elongation of the patch boundary, indicating that antimicrobial peptide could lower the line tension of the boundary edge (Fig 4A, 0.05 μM AMP). Imperfect amphipathicity (from imperfect segregation of amino acids, or from breaks in the symmetry of secondary structure motifs) was the only shared

property of these line active peptides. In contrast, the only non-line-active peptide showed perfect amphipathicity. It was therefore proposed that imperfect amphipathicity may enable AMPs to adopt to the curvature of membrane edges, stabilising and propagating the boundary, as also proposed previously[100] and as observed in other AFM studies.[87, 96]

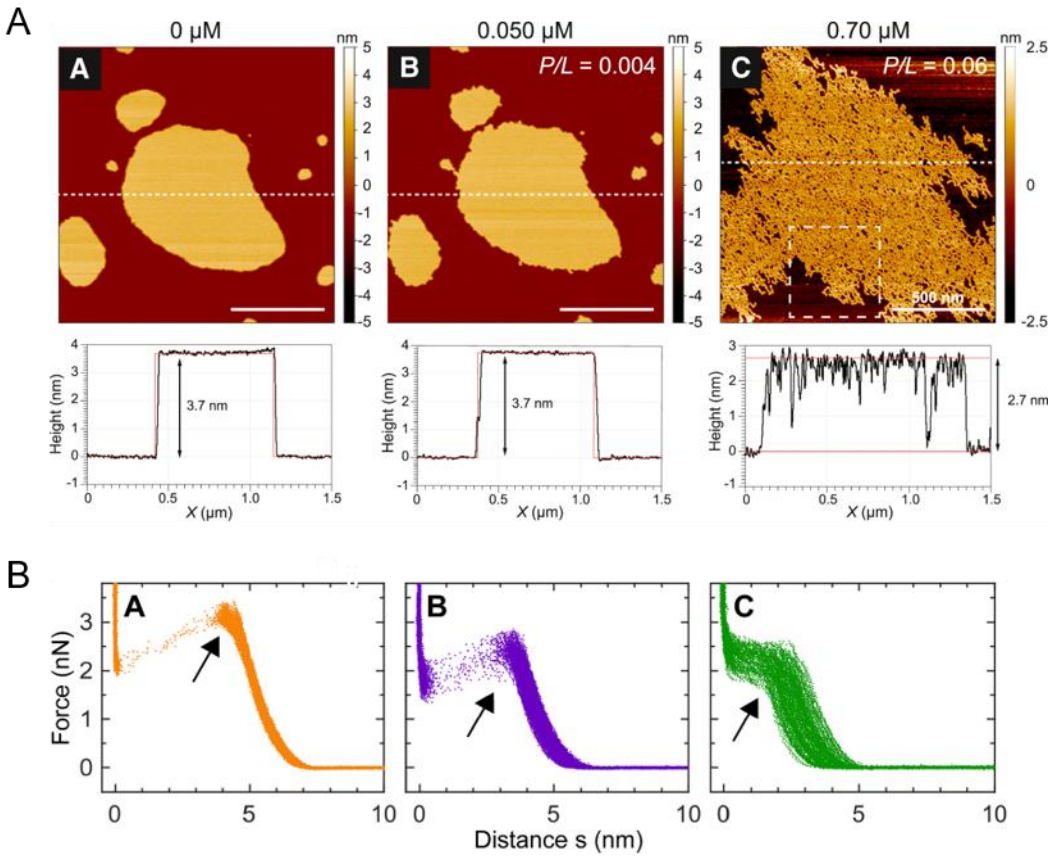

Figure 4. AFM observation of AMP disruption on supported lipid bilayers (SLBs). (A) AFM topography images showing the structural transformation of a DMPC membrane patch treated with the peptide PG-1. The patch goes from compact and smooth edged (0 μM PG-1), to extended and roughened (0.05 μM PG-1) to non-lamellar worm-like micelles (0.7 μM PG-1). Scale bar: 500 nm. Reproduced from ref. [86], with permission from Elsevier. (B) Force-distance curves of an SLB treated with the peptide M2AH: (A) 0 μM (B) 4 μM and (C) 10 μM. Black arrows indicate bilayer puncture. Reproduced from ref. [89], with permission from Elsevier.

Phase separated L_o/L_d bilayers also have inherent line tension. There is a hydrophobic mismatch between L_o and L_d phases and domains form in compact round patches to minimise the boundary length between the two phases. AMPs exhibit line-active behaviour in this environment as well: e.g., L_o domains can become extended and heterogenous in shape.[79, 101]

2.7. Mechanical destabilisation

Besides topographical imaging, AFM can be used to record force-curves, where the force on the AFM tip is measured as the tip indents into the surface. For SLBs, this results in a jump in the force curve when the AFM tip first penetrates the lipid bilayer, followed by a sharp rise in the force as the tip reaches the solid support (Fig 4B). The bilayer thickness then corresponds to the distance that the tip travels between first touching the bilayer surface and touching the solid support, providing a useful probe to quantify those membrane thinning and thickening effects that cannot be measured topographically.[89, 97] The mechanical stability of a membrane can also be measured, via the force needed to penetrate its surface. For peptide-bound membranes a much lower force is needed to puncture through the bilayer.[89, 97, 101, 102] In some cases, destabilisation of the membrane occurs at very low peptide concentrations.[97] In other cases a threshold peptide concentration is needed, below which peptide addition increases the force needed to puncture the membrane, presumably because peptide binding to the membrane surface increases the lateral pressure at the surface.[101, 102]

To date, there have been few studies comparing the relationship between bilayer stability and topographical defects formed. In one, the extent of destabilisation correlated with the number of nanoscale pits was observed.[89] In another study, destabilisation plateaued after a certain peptide concentration, despite the number of transmembrane defects continuing to increase.[97] Exact relationships between defect formation and mechanical integrity of the membrane requires more investigation.

2.8. Multiple modes of membrane disruption

In general, single peptide sequences are observed to exert single modes of membrane disruption. The mode itself can change in different environmental conditions (discussed in section 4), but multiple simultaneous modes are not usually induced. Recently however, two multi-helical peptides were shown to cause multi-modal membrane disruption.[103] In both cases, the peptides induce localised regions of membrane thinning at the same time as inducing transmembrane channels. This may indicate that more complex, multi-helical structures can support multi-modal mechanisms, and invites further investigation.

3. Dynamics of membrane disruption

An important advantage of AFM is that it can monitor interactions between model membranes and antimicrobial peptides as a function of time. From time-resolved AFM studies, it has become clear that peptide-lipid interactions are highly dynamic and that defects can develop, expand and change.

3.1. Expanding defects

Rakowska et al hypothesised that antimicrobial pores can expand indefinitely over time and provided the first evidence of a pore expansion mechanism.[104] Over a period of 2 hours, heterogeneous pores

formed, expanded and merged to the point of complete membrane disintegration. Upon formation, pores act as sites of peptide recruitment as peptide affinity to membrane edges is favoured and drives peptide migration from a surface bound state to the pore edge. An increasing electrostatic repulsion between cationic AMP at the pore edges will then drive expansion of the pores. Lipid micellization and removal accompanies the process. A complementary observation was made for melittin (Fig 5A).[79] It was proposed that defect lining lipids are metastable and have a low free energy barrier ΔG for being removed to the aqueous phase. When they are extracted, the hydrophobic tails of bulk phase lipids are left exposed, causing a rapid re-arrangement of nearby lipids and peptide molecules to line the pore that expanded. This process repeats as more lipid is removed to the aqueous phase.

The timescale of defect expansion is dependent on both lipid composition, the type of AMP and its concentration. Defects seem to grow faster in shorter chain phospholipids, while the addition of cholesterol slows defect growth.[79] Heath et al used high-speed AFM and in-situ injection to follow the initial formation of membrane defects, and found that the process is faster when anionic lipids are present,[105] while De Santis et al showed that pre-concentrating the AMP into self-assembled capsids results in rapidly expanding membrane pores that completely solubilise the SLB in under 5 min (Fig 5B).[106]

In most of these cases, defects grew in a heterogeneous way. A highly organised expansion was also observed. Disruption defects grew in a fractal like manner (Fig 5C).[105] The morphology of the fractal defects can be modelled by two-dimensional diffusion-limited aggregation. In this model, particles with Brownian motion coalesce when they come into contact with an aggregate. Because coalescence is immediate, particles are unable to diffuse to the centre of the aggregate. Instead, they become trapped by the outer edges of the aggregate, leading to fractal growth. Immediate incorporation of peptide to a defect boundary edge is not physically realistic, so a “sticking probability” was added to this model: the probability of peptide binding to a defect edge and subsequently removing lipid. With a high sticking probability, branched fractal morphologies form. At lower sticking probabilities the peptide has a greater chance of diffusing towards the centre of the aggregate, and defects become rounded with no branches.[105] This provides a continuum for understanding how defects might grow, linking fractal growth to heterogeneous pore expansion.

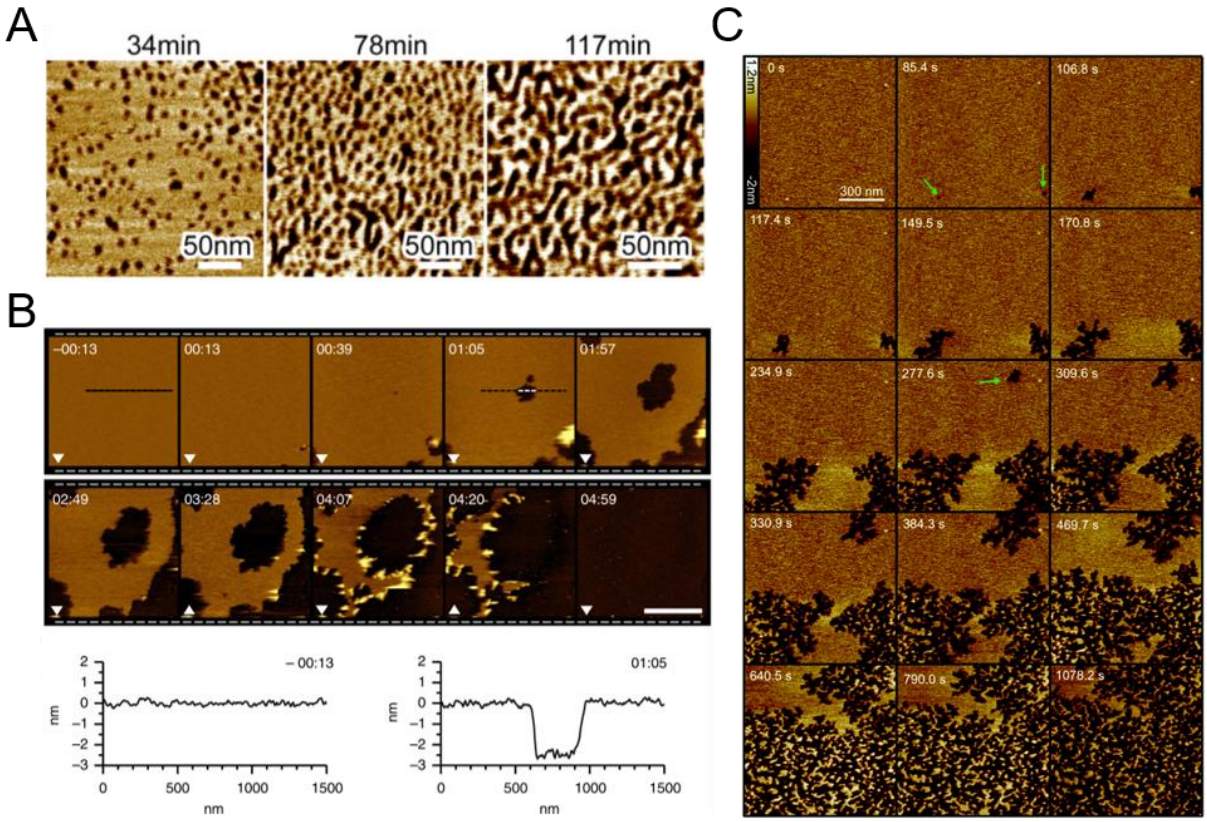

Figure 5. Time resolved AFM showing the expansion of AMP defects on supported lipid bilayers (SLBs). (A) AFM topography images showing melittin induced poration of a SLB, with pores growing and merging over 2 hours. Reproduced from ref. [79], with permission, © 2016 American Chemical Society. (B) Fast scanning AFM topography images showing how self-assembled peptide capsids solubilise a SLB in under 5 min. Scale bar 1 μm. Reproduced from ref. [106], licensed under CC BY 4.0. (C) Fast-scanning AFM images showing the formation and expansion of Smp43-induced bilayer defects. Green arrows indicate the first appearance of defects. Reproduced from ref. [105], licensed under CC BY-NC 3.0, Published by The Royal Society of Chemistry.

3.2. Metastable defects

With its high spatiotemporal resolution, time-resolved AFM can access the other end of the spectrum and help study defects that can get smaller, and even disappear. By disabling the slow axis, AFM can be used to scan laterally back and forth in the same y position with a high temporal resolution. Kim et al used this to show that a synthetic AMP pHD108 can form both stable and metastable pores, the latter fluctuating on sub-second timescales.[107] With a temporal resolution of 0.3 s, some pore like features remain unchanged, whereas others are highly dynamic and appear, disappear and re-appear. These observations support previous proposals of membrane recovery and pore sealing.[108] Similarly, AFM is equipped to tackle defect transitions, as was observed for macrolittin peptides (Fig 6A).[109] Sequential image analysis showed that pores depths fluctuate suggesting lipid re-filling

effects. The timescale for such fluctuations appeared to be slower than 0.2 s (trace to retrace) and faster than 3 min (frame to frame).

3.3. Self-assembled peptide systems

Resolving individual peptide molecules is an anticipated milestone for AFM methodologies in this context, but has remained elusive so far. However, self-assembled antimicrobial systems are visible by AFM. [106, 110, 111] For example, the dynamic membrane activity of a peptide which assembles into a capsid-like structure could be resolved.[111] These pseudocapsids can be visualised to bind to the membrane surface with a nanoscale precision, where they then re-assembles in the bilayer forming lesions and pores (Fig 6B).

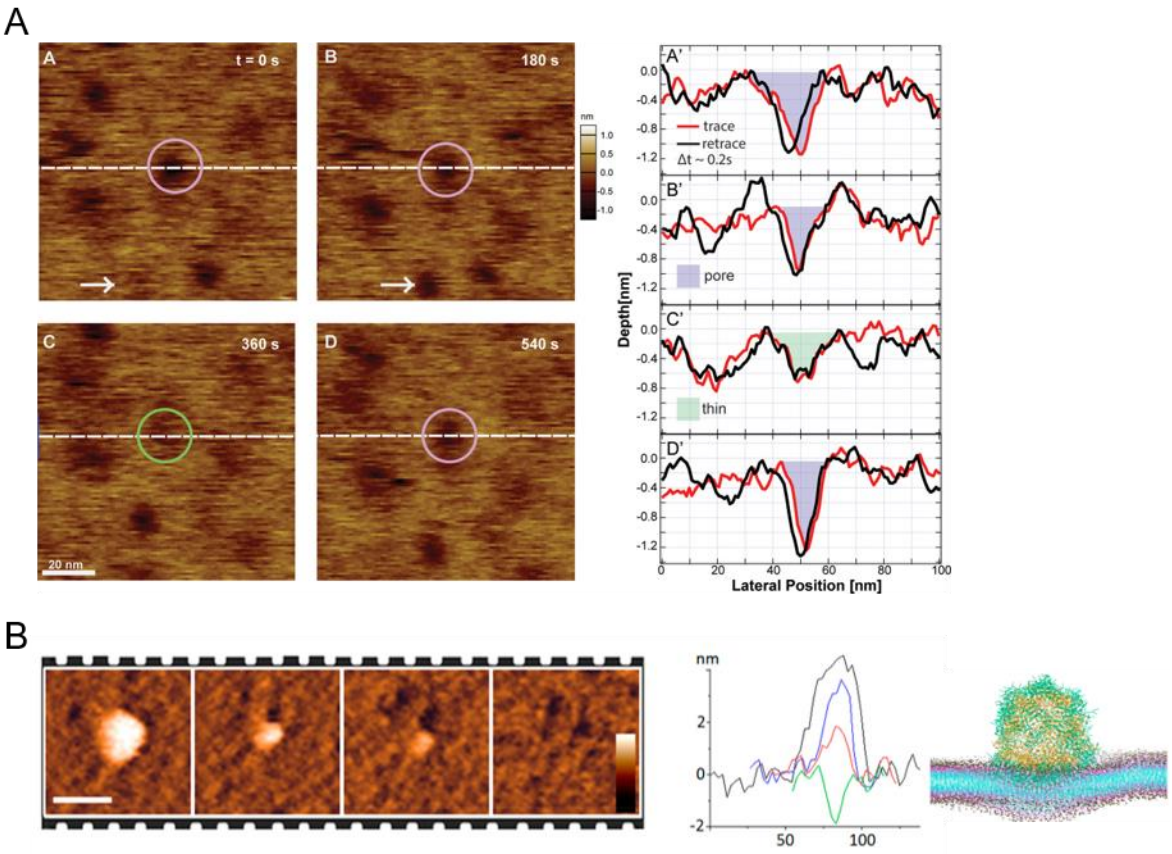

Figure 6. Time-resolved AMP-induced membrane disruption. (A) AFM topography images showing the dynamic transitions of MelP5 induced membrane defects, with cross sections shown. Reproduced from ref. [90], with permission, © 2018 American Chemical Society. (B) AFM topography images showing the binding of a self-assembled peptide capsule and its disintegration into the SLB. Images taken at 5 min intervals, scale bar 50 nm, height bar 10 nm. Cross sections and a snapshot of coarse-grain MD simulations of the capsule binding to a bilayer also shown. Reproduced from ref. [111], licensed under ACS AuthorChoice, with permission from ACS.

Recently, Shen et al designed an AMP that self-assembles on the membrane surface itself.[112] This peptide exists as a monomer in solution at pH 7.4 but assembles into nanofibers on anionic membranes. The process is selective for anionic lipids, and no self-assembly was observed on zwitterionic membranes. Self-assembly enhanced the ability of the AMP to disrupt the membrane, which is consistent with earlier reports that self-assembly of moderate antimicrobials into extended fibrillar structures can modulate antimicrobial effects enhancing them to the point of effective biofilm resistance.[113, 114]

Whilst substantial poration of the anionic membrane was observed, no defects were observed for the zwitterionic membrane, or for a control sequence which was unable to assemble. Sarkar et al designed a self-assembling AMP-based hydrogel which assembles into a fibrous matrix that can coat the surface of bacterial cells, resulting in potent disruption and cell lysis.[115] Self-assembly can reduce the risk of AMP degradation and nanoscale antimicrobial assemblies hold promise as a new class of antimicrobial materials.

4. Conditions affecting antimicrobial membrane disruption

There is no standard set of experimental conditions in AFM model membrane studies. Different lipid compositions (charge, fluidity, and thickness), concentrations of peptide, timescales of imaging and aqueous environments (pH and ionic strength) are used. Each of these factors can affect the measured activity. The findings to date indicate that antimicrobial peptides can use multiple mechanisms of attack allowing them to adapt to differences in their environment.

4.1. Phospholipid length and charge

In many AFM studies, AMPs are found to cause no disruption to zwitterionic model membranes and only disrupt membranes when anionic PG or PS lipids are present.[80] In cases where AMPs form defects in both zwitterionic and anionic membranes, negative charge often increases the kinetics of defect formation, and the size of the defects formed.[84, 105, 116] In some cases, the mode of action changes when anionic lipids are introduced. For example, for a synthetic AMP construct HDM1 inspired by helminth host defence molecules, it was found that the peptide causes thinning of zwitterionic DLPC-only bilayers, but poration when on bilayers that also contain anionic DLPG,[80] whereas magainin 2 can solubilise DMPC bilayers but forms discrete pores in DMPC/PG bilayers.[87] There are also examples of peptides that appear to function independently of the net membrane charge. This tends to be the case for hydrophobic peptides where defect formation is driven by hydrophobic interactions with lipid chains rather than by electrostatic interactions with phospholipid heads.[79, 89]

Defect formation can be dependent on the length of acyl chains, though this is seldom observed. Longer chains may result in reduced activity, with smaller defects observed and slower formation.[79,

117] This is in agreement with other studies that suggest thicker bilayers, require a higher concentration of peptide to exert a disruptive effect.[118]

4.2. Cholesterol content and lipid fluidity

The fluidity of the bilayer has a significant effect on peptide activity. Addition of cholesterol to L_d bilayers reduces their fluidity by increasing the lipid order. Such L_d/chol bilayers can show resistance to peptide insertion, presumably due to an increase in the free energy barrier for incorporating the peptides between the lipid chains. For example, poration of L_d membranes by the AMP PG-1 is reduced 10-fold by increasing the cholesterol content from 0% to 15%, and poration is completely prevented at 30%.[117] In addition, cholesterol can act as a direct competitor for peptide-lipid hydrophobic interactions and will also increase the thickness of a lipid bilayer which in-turn can reduce peptide activity. Eukaryotic cell membranes contain up to 40 % cholesterol, [119] and this may provide some protection against AMPs.

In experiments with phase separated L_o/L_d bilayers, AFM can directly compare peptide modes of action on L_o and L_d domains, with poration defects generally observed to preferentially occur in the L_d domains.[79] Such poration in the L_d domains leads to an increase in the area of the L_o domains, presumably because the peptide can selectively extract disordered lipid, thus changing the equilibrium phase distribution. Phase separated S_o/L_d bilayers enable a similar investigation of peptide preference for lipid fluidity. Defects are often observed in the liquid-phase domains with expansion of gel domains.[120]

Cholesterol exerts the opposite effect on gel-state S_o bilayers, disrupting the highly ordered packing and resulting in increased lipid fluidity. Such S_o/chol bilayers are often more susceptible to peptide insertion than S_o bilayers. For example, the pore-forming peptide melittin was more active against gel-state DMPC/PG/chol then against DMPC/PG.[96] Interestingly, a completely different disruption mechanism was observed for the DMPC/PG/chol. This demonstrates that lipid fluidity can change not just the strength of interaction, but also the interaction mechanism itself. In agreement with this, a recent AFM study of phase separated S_o/L_d DPPC/DOPC bilayers showed that a synthetic AMP construct exerted very different disruption effects on the fluid and gel state lipid.[121]

Taken together, peptide insertion appears more effective in (more) fluid membranes. Significant parts of the eukaryotic membrane can exist in a liquid-ordered, L_o state[22] and although there is emerging evidence that L_o domains can form in bacterial membranes, the lack of high quantities of L_o-promoting lipids and hydrophobic molecules (such as cholesterol and sphingomyelin) means it is generally considered to be more disordered.[25] This may well contribute to the selectivity of antimicrobial peptides for bacterial cells. In parallel, peptides that target eukaryotic membranes such as the influenza virus M2 amphipathic helix, and the human protein α-synuclein, have been observed

to be more active in more ordered, cholesterol containing bilayers.[84, 89] Membrane-active peptides seem to have developed inherent specificity for the fluidity of their target membrane.

4.3. Peptide concentration

In most AFM studies the extent of defect coverage and the speed of formation were proportional to peptide concentrations, with higher concentrations leading to more defects that formed faster.[84, 88, 120] In these cases, the mechanism of disruption remains the same and only the kinetics of formation and expansion change.

In some AFM studies, however, the mechanism can depend on peptide concentration. For toroidal pore forming peptides, a threshold concentration of AMP is required to bind to the surface before observable pores are formed, and at higher concentrations complete membrane solubilisation can occur.[80, 90] For the line-active peptides, membrane disruption begins with boundary extension, and with increasing concentration, edge defects appear and grow, followed by bulk defects and an induction of non-lamellar phase culminating with the appearance of worm-like micelles (Fig 4A).[86] All peptides in that study follow the same trend, but the concentration required for each defect type varies by over three orders of magnitude (from 0.1 μM to 70 μM). It is difficult to assess what is a physiologically relevant concentration range in general for AFM studies. *In vivo*, the human AMP LL-37 is found at sites of infection at concentrations of up to 1.1 μM.[122] However, how this relates to the active concentration at the membrane is not clear. It could be lower than the bulk concentration due to the presence of multiple alternative binding partners that can sequester peptide molecules, or higher due to active recruitment of AMPs to the anionic bacterial surface. A more practical consideration is that at higher concentrations, complete membrane solubilisation tends to occur before any detailed information about specific peptide-lipid interactions can be recorded, and most AFM studies use concentrations lower than 1 μM.

4.4. pH and ionic strength

Finally, sample solution, its pH and ionic strength, can have a significant impact on membrane disruption mechanisms. Changes in protonation states of amino acids may affect peptide-peptide and peptide-lipid electrostatic interactions, as in pH-dependent AMPs that are only active at pH < 5,[107] suggesting membrane disruption is sensitive to pH. Most AFM studies are conducted in buffer solutions close to physiological pH.

The ionic strength of the imaging solution will also alter the mechanism of peptide attack. For untreated SLBs, the stability of the bilayer decreases significantly with decreasing ionic strength (demonstrated for 150 mM to 0 mM NaCl solution).[123] There is no standard imaging solution used across AFM studies of peptide disruption. Many use physiological salt conditions (100-150 mM NaCl), but some studies are done at a much lower ionic strength (10-20 mM). With already

destabilised SLBs, such conditions are likely to enhance peptide-induced disruption. Furthermore, membrane defects are often an equilibrium state as opposed to an irreversible change, and as repeatedly demonstrated throughout this review, changes to environmental conditions can change the mode of disruption.

5. Outlook

5.1. Improved model systems

As used in AFM experiments, SLBs obviously differ from physiological membranes by being in close proximity to the solid support. The hydration layer between the lower leaflet lipids and the underlying support (around 1 nm thick)[124] conserves lipid fluidity and dynamics, but – depending on lipid composition – the diffusion coefficient in SLBs can be around two times smaller than in free standing bilayers such as GUVs.[125] This is thought to be due to atomic scale corrugation on the substrate surface.[126] Furthermore, binding of the AMP to the lower leaflet lipids may be influenced by the solid support. Model membranes such as tethered and polymer-cushioned bilayers have been used to introduce a spacer between the solid support and the lipids, reducing the influence of the substrate.[127, 128] Recent advances in the preparation of floating bilayers, with tuneable aqueous layers of 10-30 nm represent more accurate biomimetic models to date (Fig 7A), and their use for membrane disruption studies is likely to increase if they lead to significantly different results on AMP-membrane interactions compared with SLBs.[129] However, the compatibility of these systems with AFM imaging is yet to be confirmed. Another approach is pore-spanning bilayers, which retain the free-standing nature but introduce solid support at the pore edges. Such systems can be imaged by AFM and have been prepared with diameters of up to 600 nm, yet it remains to be established what resolution can be obtained in imaging AMP-induced membrane disruption.[130]

Besides simple phospholipid mixtures, SLBs can be formed with natural lipid extracts from both bacterial and eukaryotic membranes. These can be total lipid extracts (TLE), which contain a broad variety of lipids including gangliosides and cholesterol, or polar lipid extracts (PLE), which removes the non-polar lipid component. SLBs have successfully been formed from a wide variety of lipid extracts with examples ranging from porcine brain TLE[131] to bovine heart TLE[132]. Bacterial lipid extracts can be more challenging due to high quantities of non-bilayer forming lipids such as PE, and negatively charged lipids that repel the surface and require addition of e.g. Ca^{2+} ions,[133] but SLB formation is routinely achievable, with *E.coli* TLE and PLE most commonly used.[134, 135] AFM analysis of pore-forming proteins and pore-forming toxins have been conducted on such bacterial lipid extracts[136, 137] but the use of lipid extracts SLBs in AFM studies of peptide-induced membrane disruption has been limited, despite being used by other techniques (see e.g. ref. [138, 139]). There is a current scarcity in the literature of studies on the characterisation of AMPs on more complex lipid mixtures.

Entire native membranes, including the protein component, could also be extracted and adsorbed on mica substrates for AFM imaging, such as rod outer segment (ROS) disc membranes and purple membranes.[140, 141] Until now, membranes have generally been ruptured and flattened to allow adsorption to the mica surface, but this process will affect protein organisation and may result in loss of protein molecules. By using high-speed AFM with short cantilevers and optimised buffer conditions, the tip-sample interactions were reduced enough to allow high resolution imaging of a vesicular bacterial chromatophore, i.e., a curved native membrane, despite it being supported only by the fluid in the vesicle and the mechanical properties of the membrane itself (Fig 7B) [142]. Such methodological advances open new avenues for future studies on curved native membranes and protein-rich vesicles.

Membrane-curvature alone may well influence peptide-lipid interactions yet is not present in (planar) SLBs. To assess its effect in isolation, parallel studies on simple lipid vesicles and corresponding SLBs of the same lipid composition should be conducted. Considerable success has been had in imaging the surface of intact vesicles adsorbed onto solid supports in high-resolution by AFM (as reviewed by ref. [143]). Such systems have yet to be used to study peptide-induced disruption, but could provide a well-defined comparison to better understand the effect of membrane curvature.

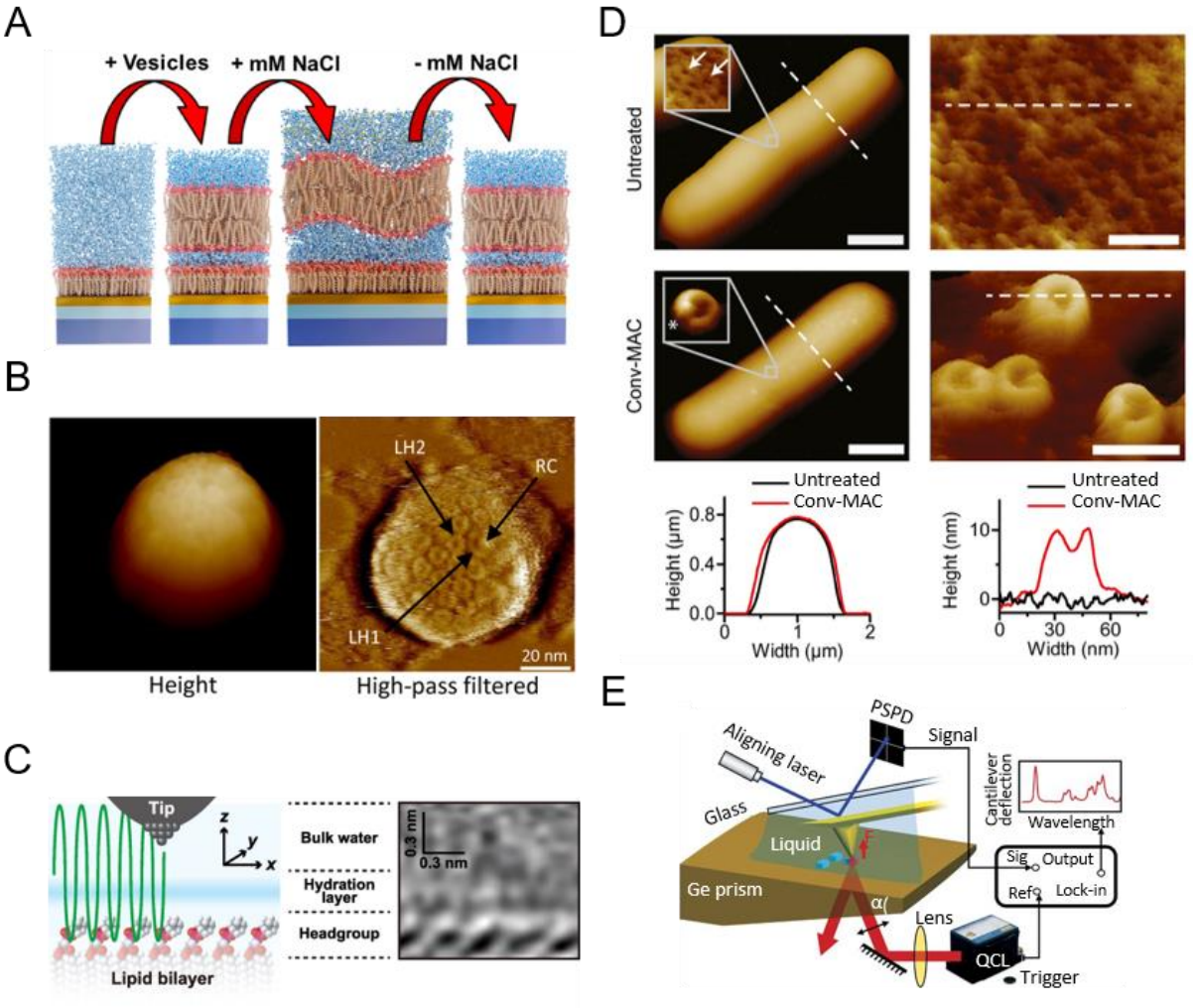

Figure 7. Future directions for the application of AFM to understanding AMP-induced membrane disruption. (A) Fluid phase floating membranes can be prepared and tuned. Reproduced from ref. [129], with permission © 2019 American Chemical Society. (B) AFM topography image of the protein organisation in a vesicular bacterial chromatophore. Reproduced from ref. [142], licensed under ACS AuthorChoice, with permission from ACS. (C) High resolution 3D FM-AFM can resolve the lipid head groups and hydration layers at the surface of a gel-state lipid bilayer. Reproduced from ref. [30], with permission, © 2012 American Chemical Society. (D) High-resolution imaging of live E. *coli* BL21 cells, comparing the surface topography of untreated cells and C5-C9 (Conv-MAC)-treated cells. Scale bars 800 nm (left) and 30 nm (right). Reproduced from ref. [144], licensed under CC BY 4.0. (E) Experimental setup for high-sensitivity infrared vibrational nanospectroscopy in water. Reproduced from ref. [145], licensed under CC BY-NC-SA 4.0.

5.2. Resolving peptide molecules

Advances in HS-AFM have enabled proteins to be resolved in model membranes with greatly improved spatiotemporal resolution (nanometre, sub-second) and the characterisation of protein conformational dynamics is now possible.[3, 146] For example, individual glutamate transporters

were recently observed switching between an outward facing and inward facing conformation.[147] Advances in AFM technologies have also enabled the characterisation of protein supramolecular structures, including bax and pore-forming proteins, which oligomerise into well-defined structures in lipid bilayers, while individual protein subunits, oligomerisation states, and assembly kinetics can all be resolved.[18, 137, 148–151] Similarly, Aβ oligomers which disrupt neuronal membranes were resolved by HS-AFM during their membrane interaction.[152] This enabled the identification of lipid compositions that promote oligomer binding, those that inhibit oligomer binding, and those that promote both binding and disruption.

This level of detail has not yet been achieved for AMP-membrane interactions. These peptides are smaller and more disordered, and thus harder to resolve by AFM. It remains challenging to develop instrumentation and appropriate sample preparations that would enable individual peptides to be imaged during membrane disruption. Frequency-modulation AFM (FM-AFM) has previously been used to resolve individual gel-state lipid molecules in an aqueous environment (Fig 7C).[30] Restricting peptide mobility and phospholipids following membrane disruption, e.g., through temperature control, may allow higher resolution imaging at defect edges. Furthermore, as the temporal resolution of HS-AFM improves, peptide monomers may yet be resolvable.[146]

5.3. From model membranes to live cell studies

Reconstituted phospholipid bilayers have enabled the visualisation of effects caused by peptide binding to membranes. However, it remains unclear to what extent these results can be extrapolated to interactions that take place at the membrane surface *in vivo*. Membrane remodelling can strongly depend on phospholipid composition, thickness and fluidity. The lipid composition in model lipid bilayers does not reproduce the complexity of live biomembranes, also including integral and transmembrane proteins at high densities.

Detailed mechanistic studies of peptide-induced membrane disruption using live pathogens remain limited. Confocal studies with fluorescently labelled peptides were used to localise AMP distribution across the cell,[153] and electron microscopy is still used to image the overall effect of peptide treatment on cell surfaces.[154] There have been multiple AFM studies of bacterial, fungal and cancerous cells using dried samples.[155–164] These studies rely on capturing snapshots of cells after peptide treatment, attempting to visualise membrane disruption and preferential target sites in cells, e.g. at a higher concentration of negatively charged cardiolipin in *E. coli*. Alternatively, glutaraldehyde or formaldehyde are used to fix cells at different incubation times. For example, melittin could be observed to remodel the cellular morphology of gastric cancer cells within the first minute of peptide treatment.[165] However, these experimental conditions are subject to potential artefacts due to drying and fixation, inaccurately fixed time points and failure to access the dynamics of disruption or pore growth.

AFM performed in liquid and using live cells overcomes these shortcomings, but imaging cells live comes with its own challenges. The cells must be immobilised without affecting their viability, the imaging force must be low enough to avoid cell damage, but high enough to maintain resolution, and unlike the flat surface of model membranes, cells have large inherent variability in surface topography. Despite these difficulties, live-cell studies have been attempted.[166–173] These studies focused on general changes across the membrane surface, as the spatial resolution was not as high as for model membranes. For example, Fantner et al imaged surface roughening of E. *coli* cells after peptide treatment, correlating the kinetics of roughening with cell death.[173] Thanks to improvements in immobilisation protocols and AFM technology, it is now possible to image the surface of live bacteria at a spatial resolution that is comparable to that obtained on to SLBs (Fig 7D).[144, 174, 175] It may now be possible to visualise local peptide-membrane interactions under conditions that better mimic native environments.

Force spectroscopy studies can also be used to investigate the mechanical effects of AMPs on live pathogens. For example, functionalisation of the AFM tip with an AMP can enable single peptide-cell interactions to be measured,[162] and force-distance curves revealed that magainin dramatically decreased the turgor pressure of E. *coli* cells.[166] Furthermore, the development of multiparametric imaging enables simultaneous mapping of the mechanical properties and surface topography of live cells at the speed of conventional imaging.[1, 176–178] This is yet to be used to investigate the mechanical effect of antimicrobial peptides on the pathogen cell envelope in real-time.

5.4. Combinatory AFM

AFM is a surface technique that provides no chemical identification. The development of correlative approaches will significantly increase our ability to characterise AMP-membrane interactions both with live cells and with model-membranes. Advances in this area have been made starting with the SLB work by Rakowska et al.[104] Chemical information on the same samples imaged by AFM could be obtained by nano-scale secondary ion mass spectrometry to elucidate differential antimicrobial mechanisms in reconstituted membranes[179], and increasingly also in fixed cells. Single molecule localisation microscopy (SMLM) combined with AFM was used to image live E. *coli* cells expressing the fusion protein RNP-mEOS2.[180] AFM revealed the morphology of the bacterial surface, and SMLM revealed the spatial distribution of the fusion protein. This suggests that topographical features observed by AFM could also be identified chemically. Finally, continued advances in the resolution and sensitivity of in-liquid AFM-IR (Fig 7E) is progressing towards the goal of simultaneous chemical and topographical imaging at nanometre resolution.[145, 181]

6. Conclusions

Over the past decade, AFM has proven to be a powerful tool to advance our understanding of membrane disruption mechanisms and provide new insights into the structure-activity relationships of

host defence peptides. Direct visualisation of pore formation has allowed us to identify and distinguish various modes of membrane disruption and to relate these to specific amino acid sequences and variations in experimental conditions. Time-resolved studies have revealed the dynamic and versatile nature of peptide-membrane interactions. Reconstituted membranes have helped to obtain a level of detail that thus far would have been impractical to achieve on live cells due to their complexity, and have facilitated the analysis of factors that enhance or reduce peptide activity. More recently, advances in live-cell imaging have started allowing the extension of such experiments to native membrane systems. Finally, for both model and live-cell systems, future improvements in spatial, temporal and even chemical resolution of AFM methodologies will undoubtedly continue to push the boundaries of traditional concepts to a better appreciation of biological processes occurring in and at biomembrane interfaces.

7. Acknowledgements

The authors acknowledge past and present members of the Ryadnov and Hoogenboom labs for advice and discussions. This work has been funded by the UK Department for Business, Energy and Industrial Strategy, Innovate UK (grant: 103358), and the UK Biotechnology and Biological Sciences, and Medical Research Councils (BBSRC and MRC grants: BB/N015487/1, BB/J021474/1 and MR/R000328/1).

1. Dufrêne YF, Ando T, Garcia R, Alsteens D, Martinez-Martin D, Engel A, Gerber C, Müller DJ (2017) Imaging modes of atomic force microscopy for application in molecular and cell biology. Nat Nanotechnol 12:295–307 . https://doi.org/10.1038/nnano.2017.45

2. Ando T, Uchihashi T, Scheuring S (2014) Filming Biomolecular Processes by High-Speed Atomic Force Microscopy. Chem Rev 114:3120–3188 . https://doi.org/10.1021/cr4003837

3. Ando T (2018) High-speed atomic force microscopy and its future prospects. Biophys Rev 10:285–292 . https://doi.org/10.1007/s12551-017-0356-5

4. Krieg M, Fläschner G, Alsteens D, Gaub BM, Roos WH, Wuite GJL, Gaub HE, Gerber C, Dufrêne YF, Müller DJ (2019) Atomic force microscopy-based mechanobiology. Nat Rev Phys 1:41–57 . https://doi.org/10.1038/s42254-018-0001-7

5. Gerber C, Lang HP (2006) How the doors to the nanoworld were opened. Nat Nanotechnol 1:3–5 . https://doi.org/10.1038/nnano.2006.70

6. Cattin CJ, Düggelin M, Martinez-Martin D, Gerber C, Müller DJ, Stewart MP (2015)

Mechanical control of mitotic progression in single animal cells. Proc Natl Acad Sci U S A 112:11258–63 . https://doi.org/10.1073/pnas.1502029112

7. Garcia-Manyes S, Redondo-Morata L, Oncins G, Sanz F (2010) Nanomechanics of Lipid Bilayers: Heads or Tails? J Am Chem Soc 132:12874–12886 . https://doi.org/10.1021/ja1002185

8. Picas L, Milhiet P-E, Hernández-Borrell J (2012) Atomic force microscopy: A versatile tool to probe the physical and chemical properties of supported membranes at the nanoscale. Chem Phys Lipids 165:845–860 . https://doi.org/10.1016/J.CHEMPHYSLIP.2012.10.005

9. Connell SD, Smith DA (2006) The atomic force microscope as a tool for studying phase separation in lipid membranes (Review). Mol Membr Biol 23:17–28 . https://doi.org/10.1080/09687860500501158

10. Richter RP, Bérat R, Brisson AR (2006) Formation of Solid-Supported Lipid Bilayers: An Integrated View. Langmuir 22:3497–3505 . https://doi.org/10.1021/LA052687C

11. Gosvami NN, Parsons E, Marcovich C, Berkowitz ML, Hoogenboom BW, Perkin S (2012) Resolving the structure of a model hydrophobic surface: DODAB monolayers on mica. RSC Adv 2:4181 . https://doi.org/10.1039/c2ra20108a

12. Al-Rekabi Z, Contera S (2018) Multifrequency AFM reveals lipid membrane mechanical properties and the effect of cholesterol in modulating viscoelasticity. Proc Natl Acad Sci U S A 115:2658–2663 . https://doi.org/10.1073/pnas.1719065115

13. Ulman A (1991) An Introduction to Ultrathin Organic Films. Elsevier

14. Brian AA, McConnell HM (1984) Allogeneic stimulation of cytotoxic T cells by supported planar membranes. Proc Natl Acad Sci U S A 81:6159–63 . https://doi.org/10.1073/PNAS.81.19.6159

15. McConnell HM, Watts TH, Weis RM, Brian AA (1986) Supported planar membranes in studies of cell-cell recognition in the immune system. Biochim Biophys Acta - Rev Biomembr 864:95–106 . https://doi.org/10.1016/0304-4157(86)90016-X

16. Morandat S, Azouzi S, Beauvais E, Mastouri A, El Kirat K (2013) Atomic force microscopy of model lipid membranes. Anal Bioanal Chem 405:1445–1461 . https://doi.org/10.1007/s00216-012-6383-y

17. Hoogenboom BW (2012) AFM in Liquids. In: Bhushan B (ed) Encyclopedia of Nanotechnology. Springer Netherlands, Dordrecht, pp 83–89

18. Rudd-Schmidt JA, Hodel AW, Noori T, Lopez JA, Cho H-J, Verschoor S, Ciccone A, Trapani

JA, Hoogenboom BW, Voskoboinik I (2019) Lipid order and charge protect killer T cells from accidental death. Nat Commun 10:5396 . https://doi.org/10.1038/s41467-019-13385-x

19. van Meer G, Voelker DR, Feigenson GW (2008) Membrane lipids: Where they are and how they behave. Nat Rev Mol Cell Biol 9:112–124 . https://doi.org/10.1038/nrm2330

20. Norlén L (2001) Skin barrier structure and function: the single gel phase model. J Invest Dermatol 117:830–6 . https://doi.org/10.1038/jid.2001.1

21. Mouritsen OG, Zuckermann MJ (2004) What's so special about cholesterol? Lipids 39:1101–1113 . https://doi.org/10.1007/s11745-004-1336-x

22. Owen DM, Williamson DJ, Magenau A, Gaus K (2012) Sub-resolution lipid domains exist in the plasma membrane and regulate protein diffusion and distribution. Nat Commun 3:1256 . https://doi.org/10.1038/ncomms2273

23. Connell SD, Heath G, Olmsted PD, Kisil A (2013) Critical point fluctuations in supported lipid membranes. Faraday Discuss 161:91–111 . https://doi.org/10.1039/C2FD20119D

24. Matsumoto K, Kusaka J, Nishibori A, Hara H (2006) Lipid domains in bacterial membranes. Mol Microbiol 61:1110–1117 . https://doi.org/10.1111/j.1365-2958.2006.05317.x

25. Strahl H, Errington J (2017) Bacterial Membranes: Structure, Domains, and Function. Annu Rev Microbiol 71:519–538 . https://doi.org/10.1146/annurev-micro-102215-095630

26. Jia Z, O'Mara ML, Zuegg J, Cooper MA, Mark AE (2011) The effect of environment on the recognition and binding of vancomycin to native and resistant forms of lipid II. Biophys J 101:2684–92 . https://doi.org/10.1016/j.bpj.2011.10.047

27. Sáenz JP, Grosser D, Bradley AS, Lagny TJ, Lavrynenko O, Broda M, Simons K (2015) Hopanoids as functional analogues of cholesterol in bacterial membranes. Proc Natl Acad Sci U S A 112:11971–6 . https://doi.org/10.1073/pnas.1515607112

28. Honigmann A, Pralle A (2016) Compartmentalization of the Cell Membrane. J Mol Biol 428:4739–4748 . https://doi.org/10.1016/J.JMB.2016.09.022

29. Mileykovskaya E, Dowhan W (2000) Visualization of phospholipid domains in Escherichia coli by using the cardiolipin-specific fluorescent dye 10-N-nonyl acridine orange. J Bacteriol 182:1172–5 . https://doi.org/10.1128/jb.182.4.1172-1175.2000

30. Asakawa H, Yoshioka S, Nishimura K, Fukuma T (2012) Spatial Distribution of Lipid Headgroups and Water Molecules at Membrane/Water Interfaces Visualized by Three-Dimensional Scanning Force Microscopy. ACS Nano 6:9013–9020 . https://doi.org/10.1021/nn303229j

31. Li J, Koh J-J, Liu S, Lakshminarayanan R, Verma CS, Beuerman RW (2017) Membrane Active Antimicrobial Peptides: Translating Mechanistic Insights to Design. Front Neurosci 11:73 . https://doi.org/10.3389/fnins.2017.00073

32. Mookherjee N, Anderson MA, Haagsman HP, Davidson DJ (2020) Antimicrobial host defence peptides: functions and clinical potential. Nat Rev Drug Discov 19:311–332 . https://doi.org/10.1038/s41573-019-0058-8

33. Nielsen JE, Bjørnestad VA, Lund R (2018) Resolving the structural interactions between antimicrobial peptides and lipid membranes using small-angle scattering methods: the case of indolicidin. Soft Matter 14:8750–8763 . https://doi.org/10.1039/c8sm01888j

34. Clifton LA, Hall SCL, Mahmoudi N, Knowles TJ, Heinrich F, Lakey JH (2019) Structural Investigations of Protein-Lipid Complexes Using Neutron Scattering. Methods Mol Biol 2003:201–251 . https://doi.org/10.1007/978-1-4939-9512-7_11

35. He K, Ludtke SJ, Huang HW, Worcester DL (1995) Antimicrobial Peptide Pores in Membranes Detected by Neutron In-Plane Scattering. Biochemistry 34:15614–15618 . https://doi.org/10.1021/bi00048a002

36. Qian S, Heller WT (2011) Peptide-Induced Asymmetric Distribution of Charged Lipids in a Vesicle Bilayer Revealed by Small-Angle Neutron Scattering. J Phys Chem B 115:9831–9837 . https://doi.org/10.1021/jp204045t

37. Haney EF, Vogel HJ (2009) NMR of Antimicrobial Peptides. In: Annual Reports on NMR Spectroscopy. Academic Press, pp 1–51

38. Porcelli F, Ramamoorthy A, Barany G, Veglia G (2013) On the Role of NMR Spectroscopy for Characterization of Antimicrobial Peptides. Methods Mol Biol 1063:159–180 . https://doi.org/10.1007/978-1-62703-583-5_9

39. Bechinger B, Salnikov ES (2012) The membrane interactions of antimicrobial peptides revealed by solid-state NMR spectroscopy. Chem Phys Lipids 165:282–301 . https://doi.org/10.1016/J.CHEMPHYSLIP.2012.01.009

40. Naito A, Matsumori N, Ramamoorthy A (2018) Dynamic membrane interactions of antibacterial and antifungal biomolecules, and amyloid peptides, revealed by solid-state NMR spectroscopy. Biochim Biophys Acta - Gen Subj 1862:307–323 . https://doi.org/10.1016/J.BBAGEN.2017.06.004

41. Hartmann M, Berditsch M, Hawecker J, Ardakani MF, Gerthsen D, Ulrich AS (2010) Damage of the bacterial cell envelope by antimicrobial peptides gramicidin S and PGLa as revealed by

transmission and scanning electron microscopy. Antimicrob Agents Chemother 54:3132–42 . https://doi.org/10.1128/AAC.00124-10

42. Schneider VAF, Coorens M, Ordonez SR, Tjeerdsma-van Bokhoven JLM, Posthuma G, van Dijk A, Haagsman HP, Veldhuizen EJA (2016) Imaging the antimicrobial mechanism(s) of cathelicidin-2. Sci Rep 6:32948 . https://doi.org/10.1038/srep32948

43. Nguyen LT, Haney EF, Vogel HJ (2011) The expanding scope of antimicrobial peptide structures and their modes of action. Trends Biotechnol 29:464–472 . https://doi.org/10.1016/J.TIBTECH.2011.05.001

44. Sani MA, Separovic F (2016) How Membrane-Active Peptides Get into Lipid Membranes. Acc Chem Res 49:1130–1138 . https://doi.org/10.1021/acs.accounts.6b00074

45. Ran S, Downes A, Thorpe PE (2002) Increased exposure of anionic phospholipids on the surface of tumor blood vessels. Cancer Res 62:6132–40

46. Roudi R, Syn NL, Roudbary M (2017) Antimicrobial Peptides As Biologic and Immunotherapeutic Agents against Cancer: A Comprehensive Overview. Front Immunol 8:1320 . https://doi.org/10.3389/fimmu.2017.01320

47. Wang C, Chen Y-W, Zhang L, Gong X-G, Zhou Y, Shang D-J (2016) Melanoma cell surface-expressed phosphatidylserine as a therapeutic target for cationic anticancer peptide, temporin-1CEa. J Drug Target 24:548–556 . https://doi.org/10.3109/1061186X.2015.1113539

48. Joo H-S, Fu C-I, Otto M (2016) Bacterial strategies of resistance to antimicrobial peptides. Philos Trans R Soc B Biol Sci 371:20150292 . https://doi.org/10.1098/rstb.2015.0292

49. Ryan L, Lamarre B, Diu T, Ravi J, Judge PJ, Temple A, Carr M, Cerasoli E, Su B, Jenkinson HF, Martyna G, Crain J, Watts A, Ryadnov MG (2013) Anti-antimicrobial peptides: folding-mediated host defense antagonists. J Biol Chem 288:20162–72 . https://doi.org/10.1074/jbc.M113.459560

50. Lee T-H, Hofferek V, Separovic F, Reid GE, Aguilar M-I (2019) The role of bacterial lipid diversity and membrane properties in modulating antimicrobial peptide activity and drug resistance. Curr Opin Chem Biol 52:85–92 . https://doi.org/10.1016/J.CBPA.2019.05.025

51. Juhas M (2015) Horizontal gene transfer in human pathogens. Crit Rev Microbiol 41:101–108 . https://doi.org/10.3109/1040841X.2013.804031

52. Baltz RH (2009) Daptomycin: mechanisms of action and resistance, and biosynthetic engineering. Curr Opin Chem Biol 13:144–151 . https://doi.org/10.1016/J.CBPA.2009.02.031

53. Batoni G, Maisetta G, Brancatisano FL, Esin S, Campa M (2011) Use of Antimicrobial

Peptides Against Microbial Biofilms: Advantages and Limits. Curr Med Chem 18:256–279 . https://doi.org/10.2174/092986711794088399

54. Delattin N, Brucker K, Cremer K, Cammue B, Thevissen K (2016) Antimicrobial Peptides as a Strategy to Combat Fungal Biofilms. Curr Top Med Chem 17:604–612 . https://doi.org/10.2174/1568026616666160713142228

55. Dean RE, O'Brien LM, Thwaite JE, Fox MA, Atkins H, Ulaeto DO (2010) A carpet-based mechanism for direct antimicrobial peptide activity against vaccinia virus membranes. Peptides 31:1966–72 . https://doi.org/10.1016/j.peptides.2010.07.028

56. Brice DC, Toth Z, Diamond G (2018) LL-37 disrupts the Kaposi's sarcoma-associated herpesvirus envelope and inhibits infection in oral epithelial cells. Antiviral Res 158:25–33 . https://doi.org/10.1016/J.ANTIVIRAL.2018.07.025

57. Barlow PG, Svoboda P, Mackellar A, Nash AA, York IA, Pohl J, Davidson DJ, Donis RO (2011) Antiviral activity and increased host defense against influenza infection elicited by the human cathelicidin LL-37. PLoS One 6:e25333 . https://doi.org/10.1371/JOURNAL.PONE.0025333

58. Howell MD, Jones JF, Kisich KO, Streib JE, Gallo RL, Leung DYM (2004) Selective Killing of Vaccinia Virus by LL-37: Implications for Eczema Vaccinatum. J Immunol 172:1763–1767 . https://doi.org/10.4049/JIMMUNOL.172.3.1763

59. Wiens ME, Smith JG (2017) α-Defensin HD5 Inhibits Human Papillomavirus 16 Infection via Capsid Stabilization and Redirection to the Lysosome. MBio 8: . https://doi.org/10.1128/mBio.02304-16

60. Nguyen EK, Nemerow GR, Smith JG (2010) Direct Evidence From Single-Cell Analysis That Human {Alpha}-Defensins Block Adenovirus Uncoating to Neutralize Infection. J Virol 84:4041–4049 . https://doi.org/10.1128/JVI.02471-09

61. Guha S, Ghimire J, Wu E, Wimley WC (2019) Mechanistic Landscape of Membrane-Permeabilizing Peptides. Chem Rev 119:6040–6085 . https://doi.org/10.1021/acs.chemrev.8b00520

62. Ehrenstein G, Lecar H (1977) Electrically gated ionic channels in lipid bilayers. Q Rev Biophys 10:1–34 . https://doi.org/10.1017/S0033583500000123

63. Ludtke SJ, He K, Heller WT, Harroun TA, Yang L, Huang HW (1996) Membrane Pores Induced by Magainin. Biochemistry 35:13723–8 . https://doi.org/10.1021/BI9620621

64. Matsuzaki K, Murase O, Nobutaka F, Miyajima K (1996) An Antimicrobial Peptide, Magainin

2, Induced Rapid Flip-Flop of Phospholipids Coupled with Pore Formation and Peptide Translocation. Biochemistry 35:11361–8 . https://doi.org/10.1021/BI960016V

65. Pouny Y, Rapaport D, Mor A, Nicolas P, Shai Y (1992) Interaction of antimicrobial dermaseptin and its fluorescently labeled analogs with phospholipid membranes. Biochemistry 31:12416–12423 . https://doi.org/10.1021/bi00164a017

66. Faust JE, Yang P-Y, Huang HW (2017) Action of Antimicrobial Peptides on Bacterial and Lipid Membranes: A Direct Comparison. Biophys J 112:1663–1672 . https://doi.org/10.1016/j.bpj.2017.03.003

67. Islam MZ, Alam JM, Tamba Y, Karal MAS, Yamazaki M (2014) The single GUV method for revealing the functions of antimicrobial, pore-forming toxin, and cell-penetrating peptides or proteins. Phys Chem Chem Phys 16:15752–67 . https://doi.org/10.1039/c4cp00717d

68. Kristensen K, Henriksen JR, Andresen TL (2014) Quantification of leakage from large unilamellar lipid vesicles by fluorescence correlation spectroscopy. Biochim Biophys Acta - Biomembr 1838:2994–3002 . https://doi.org/10.1016/J.BBAMEM.2014.08.007

69. Avitabile C, D'Andrea LD, Romanelli A (2015) Circular Dichroism studies on the interactions of antimicrobial peptides with bacterial cells. Sci Rep 4:4293 . https://doi.org/10.1038/srep04293

70. Bürck J, Wadhwani P, Fanghänel S, Ulrich AS (2016) Oriented Circular Dichroism: A Method to Characterize Membrane-Active Peptides in Oriented Lipid Bilayers. Acc Chem Res 49:184–192 . https://doi.org/10.1021/acs.accounts.5b00346

71. Lipkin R, Lazaridis T (2017) Computational studies of peptide-induced membrane pore formation. Philos Trans R Soc B Biol Sci 372:20160219 . https://doi.org/10.1098/rstb.2016.0219

72. Velasco-Bolom J-L, Corzo G, Garduño-Juárez R (2018) Molecular dynamics simulation of the membrane binding and disruption mechanisms by antimicrobial scorpion venom-derived peptides. J Biomol Struct Dyn 36:2070–2084 . https://doi.org/10.1080/07391102.2017.1341340

73. Zhao L, Cao Z, Bian Y, Hu G, Wang J, Zhou Y (2018) Molecular Dynamics Simulations of Human Antimicrobial Peptide LL-37 in Model POPC and POPG Lipid Bilayers. Int J Mol Sci 19:1186 . https://doi.org/10.3390/ijms19041186

74. Petkov P, Lilkova E, Ilieva N, Litov L (2019) Self-Association of Antimicrobial Peptides: A Molecular Dynamics Simulation Study on Bombinin. Int J Mol Sci 20:5450 .

https://doi.org/10.3390/ijms20215450

75. Lai P-K, Kaznessis YN (2018) Insights into Membrane Translocation of Protegrin Antimicrobial Peptides by Multistep Molecular Dynamics Simulations. ACS Omega 3:6056–6065 . https://doi.org/10.1021/acsomega.8b00483

76. Abbasi F, Alvarez-Malmagro J, Su ZF, Leitch JJ, Lipkowski J (2018) Pore Forming Properties of Alamethicin in Negatively Charged Floating Bilayer Lipid Membranes Supported on Gold Electrodes. Langmuir 34:13754–13765 . https://doi.org/10.1021/acs.langmuir.8b02554

77. Abbasi F, Leitch JJ, Su ZF, Szymanski G, Lipkowski J (2018) Direct visualization of alamethicin ion pores formed in a floating phospholipid membrane supported on a gold electrode surface. Electrochim Acta 267:195–205 . https://doi.org/10.1016/J.ELECTACTA.2018.02.057

78. Pfeil M-P, Pyne ALB, Losasso V, Ravi J, Lamarre B, Faruqui N, Alkassem H, Hammond K, Judge PJ, Winn M, Martyna GJ, Crain J, Watts A, Hoogenboom BW, Ryadnov MG (2018) Tuneable poration: host defense peptides as sequence probes for antimicrobial mechanisms. Sci Rep 8:14926 . https://doi.org/10.1038/s41598-018-33289-y

79. Pan J, Khadka NK (2016) Kinetic Defects Induced by Melittin in Model Lipid Membranes: A Solution Atomic Force Microscopy Study. J Phys Chem B 120:4625–4634 . https://doi.org/10.1021/acs.jpcb.6b02332

80. Hammond K, Lewis H, Faruqui N, Russell C, Hoogenboom BW, Ryadnov MG (2019) Helminth Defense Molecules as Design Templates for Membrane Active Antibiotics. ACS Infect Dis 5:1471–1479 . https://doi.org/10.1021/acsinfecdis.9b00157

81. Wu Y, He K, Ludtke SJ, Huang HW (1995) X-ray diffraction study of lipid bilayer membranes interacting with amphiphilic helical peptides: diphytanoyl phosphatidylcholine with alamethicin at low concentrations. Biophys J 68:2361–2369 . https://doi.org/10.1016/S0006-3495(95)80418-2

82. Ludtke S, He K, Huang H (1995) Membrane thinning caused by magainin 2. Biochemistry 34:16764–16769 . https://doi.org/10.1021/bi00051a026

83. Mecke A, Lee D-K, Ramamoorthy A, Orr BG, Banaszak Holl MM (2005) Membrane thinning due to antimicrobial peptide binding: an atomic force microscopy study of MSI-78 in lipid bilayers. Biophys J 89:4043–50 . https://doi.org/10.1529/biophysj.105.062596

84. Pan J, Dalzini A, Khadka NK, Aryal CM, Song L (2018) Lipid Extraction by α-Synuclein Generates Semi-Transmembrane Defects and Lipoprotein Nanoparticles. ACS omega 3:9586–

9597 . https://doi.org/10.1021/acsomega.8b01462

85. Pyne A, Pfeil M-P, Bennett I, Ravi J, Iavicoli P, Lamarre B, Roethke A, Ray S, Jiang H, Bella A, Reisinger B, Yin D, Little B, Muñoz-García JC, Cerasoli E, Judge PJ, Faruqui N, Calzolai L, Henrion A, Martyna GJ, Grovenor CRM, Crain J, Hoogenboom BW, Watts A, Ryadnov MG (2017) Engineering monolayer poration for rapid exfoliation of microbial membranes. Chem Sci 8:1105–1115 . https://doi.org/10.1039/C6SC02925F

86. Henderson JM, Waring AJ, Separovic F, Lee KYC (2016) Antimicrobial Peptides Share a Common Interaction Driven by Membrane Line Tension Reduction. Biophys J 111:2176–2189 . https://doi.org/10.1016/j.bpj.2016.10.003

87. Hall K, Lee T-H, Mechler AI, Swann MJ, Aguilar M-I (2015) Real-time Measurement of Membrane Conformational States Induced by Antimicrobial Peptides: Balance Between Recovery and Lysis. Sci Rep 4:5479 . https://doi.org/10.1038/srep05479

88. Khadka NK, Aryal CM, Pan J (2018) Lipopolysaccharide-Dependent Membrane Permeation and Lipid Clustering Caused by Cyclic Lipopeptide Colistin. ACS Omega 3:17828–17834 . https://doi.org/10.1021/acsomega.8b02260

89. Pan J, Dalzini A, Song L (2019) Cholesterol and phosphatidylethanolamine lipids exert opposite effects on membrane modulations caused by the M2 amphipathic helix. Biochim Biophys Acta - Biomembr 1861:201–209 . https://doi.org/10.1016/J.BBAMEM.2018.07.013

90. Pittman AE, Marsh BP, King GM (2018) Conformations and Dynamic Transitions of a Melittin Derivative That Forms Macromolecule-Sized Pores in Lipid Bilayers. Langmuir 34:8393–8399 . https://doi.org/10.1021/acs.langmuir.8b00804

91. Oliva R, Del Vecchio P, Grimaldi A, Notomista E, Cafaro V, Pane K, Schuabb V, Winter R, Petraccone L (2019) Membrane disintegration by the antimicrobial peptide (P)GKY20: lipid segregation and domain formation. Phys Chem Chem Phys 21:3989–3998 . https://doi.org/10.1039/C8CP06280C

92. Sharma VK, Qian S (2019) Effect of an Antimicrobial Peptide on Lateral Segregation of Lipids: A Structure and Dynamics Study by Neutron Scattering. Langmuir 35:4152–4160 . https://doi.org/10.1021/acs.langmuir.8b04158

93. Epand RM (1998) Lipid polymorphism and protein–lipid interactions. Biochim Biophys Acta - Rev Biomembr 1376:353–368 . https://doi.org/10.1016/S0304-4157(98)00015-X

94. Koynova R, Caffrey M (1994) Phases and phase transitions of the hydrated phosphatidylethanolamines. Chem Phys Lipids 69:1–34 . https://doi.org/10.1016/0009-

3084(94)90024-8

95. Harrison PL, Heath GR, Johnson BRG, Abdel-Rahman MA, Strong PN, Evans SD, Miller K (2016) Phospholipid dependent mechanism of smp24, an α-helical antimicrobial peptide from scorpion venom. Biochim Biophys Acta - Biomembr 1858:2737–2744 . https://doi.org/10.1016/J.BBAMEM.2016.07.018

96. Lee T-H, Hall K, Aguilar M-I (2020) The Effect of Charge on Melittin-Induced Changes in Membrane Structure and Morphology. Aust J Chem 73:195 . https://doi.org/10.1071/CH19500

97. Pan J, Sahoo PK, Dalzini A, Hayati Z, Aryal CM, Teng P, Cai J, Rodriguez Gutierrez H, Song L (2017) Membrane Disruption Mechanism of a Prion Peptide (106−126) Investigated by Atomic Force Microscopy, Raman and Electron Paramagnetic Resonance Spectroscopy. J Phys Chem B 121:5058–5071 . https://doi.org/10.1021/acs.jpcb.7b02772

98. Cummings JE, Vanderlick TK (2007) Aggregation and hemi-fusion of anionic vesicles induced by the antimicrobial peptide cryptdin-4. Biochim Biophys Acta - Biomembr 1768:1796–1804 . https://doi.org/10.1016/J.BBAMEM.2007.04.016

99. Moiset G, Cirac AD, Stuart MCA, Marrink S-J, Sengupta D, Poolman B (2013) Dual Action of BPC194: A Membrane Active Peptide Killing Bacterial Cells. PLoS One 8:e61541 . https://doi.org/10.1371/journal.pone.0061541

100. Mihajlovic M, Lazaridis T (2012) Charge distribution and imperfect amphipathicity affect pore formation by antimicrobial peptides. Biochim Biophys Acta - Biomembr 1818:1274–1283 . https://doi.org/10.1016/J.BBAMEM.2012.01.016

101. García-Sáez AJ, Chiantia S, Salgado J, Schwille P (2007) Pore formation by a Bax-derived peptide: effect on the line tension of the membrane probed by AFM. Biophys J 93:103–12 . https://doi.org/10.1529/biophysj.106.100370

102. Marín-Medina N, Mescola A, Alessandrini A (2018) Effects of the peptide Magainin H2 on Supported Lipid Bilayers studied by different biophysical techniques. Biochim Biophys Acta - Biomembr 1860:2635–2643 . https://doi.org/10.1016/J.BBAMEM.2018.10.003

103. Hammond K, Lewis H, Halliwell S, Desriac F, Nardone B, Ravi J, Hoogenboom BW, Upton M, Derrick JP, Ryadnov MG (2020) Flowering poration – a synergistic multi-mode antibacterial mechanism by a bacteriocin fold. iScience. https://doi.org/10.1016/j.isci.2020.101423

104. Rakowska PD, Jiang H, Ray S, Pyne A, Lamarre B, Carr M, Judge PJ, Ravi J, Gerling UIM, Koksch B, Martyna GJ, Hoogenboom BW, Watts A, Crain J, Grovenor CRM, Ryadnov MG

(2013) Nanoscale imaging reveals laterally expanding antimicrobial pores in lipid bilayers. Proc Natl Acad Sci U S A 110:8918–23 . https://doi.org/10.1073/pnas.1222824110

105. Heath GR, Harrison PL, Strong PN, Evans SD, Miller K (2018) Visualization of diffusion limited antimicrobial peptide attack on supported lipid membranes. Soft Matter 14:6146–6154 . https://doi.org/10.1039/C8SM00707A

106. De Santis E, Alkassem H, Lamarre B, Faruqui N, Bella A, Noble JE, Micale N, Ray S, Burns JR, Yon AR, Hoogenboom BW, Ryadnov MG (2017) Antimicrobial peptide capsids of de novo design. Nat Commun 8:2263 . https://doi.org/10.1038/s41467-017-02475-3

107. Kim SY, Pittman AE, Zapata-Mercado E, King GM, Wimley WC, Hristova K (2019) Mechanism of Action of Peptides That Cause the pH-Triggered Macromolecular Poration of Lipid Bilayers. J Am Chem Soc 141:6706–6718 . https://doi.org/10.1021/jacs.9b01970

108. Lee T-H, N. Hall K, Aguilar M-I (2015) Antimicrobial Peptide Structure and Mechanism of Action: A Focus on the Role of Membrane Structure. Curr Top Med Chem 16:25–39 . https://doi.org/10.2174/1568026615666150703121700

109. Li S, Kim SY, Pittman AE, King GM, Wimley WC, Hristova K (2018) Potent Macromolecule-Sized Poration of Lipid Bilayers by the Macrolittins, A Synthetically Evolved Family of Pore-Forming Peptides. J Am Chem Soc 140:6441–6447 . https://doi.org/10.1021/jacs.8b03026

110. Castelletto V, de Santis E, Alkassem H, Lamarre B, Noble JE, Ray S, Bella A, Burns JR, Hoogenboom BW, Ryadnov MG (2016) Structurally plastic peptide capsules for synthetic antimicrobial viruses. Chem Sci 7:1707–1711 . https://doi.org/10.1039/C5SC03260A

111. Kepiro IE, Marzuoli I, Hammond K, Ba X, Lewis H, Shaw M, Gunnoo SB, De Santis E, Łapińska U, Pagliara S, Holmes MA, Lorenz CD, Hoogenboom BW, Fraternali F, Ryadnov MG (2020) Engineering Chirally Blind Protein Pseudocapsids into Antibacterial Persisters. ACS Nano 14:1609–1622 . https://doi.org/10.1021/acsnano.9b06814

112. Shen Z, Guo Z, Zhou L, Wang Y, Zhang J, Hu J, Zhang Y (2020) Biomembrane induced *in situ* self-assembly of peptide with enhanced antimicrobial activity. Biomater Sci 8:2031–2039 . https://doi.org/10.1039/C9BM01785B

113. Faruqui N, Bella A, Ravi J, Ray S, Lamarre B, Ryadnov MG (2014) Differentially Instructive Extracellular Protein Micro-nets. J Am Chem Soc 136:7889–7898 . https://doi.org/10.1021/ja411325c

114. Ravi J, Bella A, Correia AJ V., Lamarre B, Ryadnov MG (2015) Supramolecular

amphipathicity for probing antimicrobial propensity of host defence peptides. Phys Chem Chem Phys 17:15608–15614 . https://doi.org/10.1039/C5CP01185J

115. Sarkar B, Siddiqui Z, Nguyen PK, Dube N, Fu W, Park S, Jaisinghani S, Paul R, Kozuch SD, Deng D, Iglesias-Montoro P, Li M, Sabatino D, Perlin DS, Zhang W, Mondal J, Kumar VA (2019) Membrane-Disrupting Nanofibrous Peptide Hydrogels. ACS Biomater Sci Eng 5:4657–4670 . https://doi.org/10.1021/acsbiomaterials.9b00967

116. Leite NB, Aufderhorst-Roberts A, Palma MS, Connell SD, Neto JR, Beales PA (2015) PE and PS Lipids Synergistically Enhance Membrane Poration by a Peptide with Anticancer Properties. Biophys J 109:936–947 . https://doi.org/10.1016/J.BPJ.2015.07.033

117. Henderson JM, Iyengar NS, Lam KLH, Maldonado E, Suwatthee T, Roy I, Waring AJ, Lee KYC (2019) Beyond electrostatics: Antimicrobial peptide selectivity and the influence of cholesterol-mediated fluidity and lipid chain length on protegrin-1 activity. Biochim Biophys Acta - Biomembr 1861:182977 . https://doi.org/10.1016/J.BBAMEM.2019.04.011

118. Lee T-H, Sani M-A, Overall S, Separovic F, Aguilar M-I (2018) Effect of phosphatidylcholine bilayer thickness and molecular order on the binding of the antimicrobial peptide maculatin 1.1. Biochim Biophys Acta - Biomembr 1860:300–309 . https://doi.org/10.1016/J.BBAMEM.2017.10.007

119. van Meer G, de Kroon AIPM (2011) Lipid map of the mammalian cell. J Cell Sci 124:5–8 . https://doi.org/10.1242/jcs.071233

120. Bodescu MA, Rosenkötter F, Fritz J (2017) Time lapse AFM on vesicle formation from mixed lipid bilayers induced by the membrane–active peptide melittin. Soft Matter 13:6845–6851 . https://doi.org/10.1039/C7SM01095H

121. Lei H-Z, Tian T, Du Q, Hu J, Zhang Y (2017) Sequence-dependent interactions between model peptides and lipid bilayers. Nucl Sci Tech 28:124 . https://doi.org/10.1007/s41365-017-0280-1

122. Lai Y, Gallo RL (2009) AMPed up immunity: how antimicrobial peptides have multiple roles in immune defense. Trends Immunol 30:131–41 . https://doi.org/10.1016/j.it.2008.12.003

123. Garcia-Manyes S, Oncins G, Sanz F (2005) Effect of Ion-Binding and Chemical Phospholipid Structure on the Nanomechanics of Lipid Bilayers Studied by Force Spectroscopy. Biophys J 89:1812–1826 . https://doi.org/10.1529/BIOPHYSJ.105.064030

124. Zwang TJ, Fletcher WR, Lane TJ, Johal MS (2010) Quantification of the Layer of Hydration of a Supported Lipid Bilayer. Langmuir 26:4598–4601 . https://doi.org/10.1021/la100275v

125. Guo L, Har JY, Sankaran J, Hong Y, Kannan B, Wohland T (2008) Molecular Diffusion Measurement in Lipid Bilayers over Wide Concentration Ranges: A Comparative Study. ChemPhysChem 9:721–728 . https://doi.org/10.1002/cphc.200700611

126. Tero R (2012) Substrate Effects on the Formation Process, Structure and Physicochemical Properties of Supported Lipid Bilayers. Materials (Basel) 5:2658–2680 . https://doi.org/10.3390/ma5122658

127. Tanaka M, Sackmann E (2005) Polymer-supported membranes as models of the cell surface. Nature 437:656–663 . https://doi.org/10.1038/nature04164

128. Andersson J, Köper I (2016) Tethered and Polymer Supported Bilayer Lipid Membranes: Structure and Function. Membranes (Basel) 6:30 . https://doi.org/10.3390/membranes6020030

129. Clifton LA, Paracini N, Hughes A V., Lakey JH, Steinke N-J, Cooper JFK, Gavutis M, Skoda MWA (2019) Self-Assembled Fluid Phase Floating Membranes with Tunable Water Interlayers. Langmuir 35:13735–13744 . https://doi.org/10.1021/acs.langmuir.9b02350

130. Steinem C (2015) Mechanics of lipid bilayers: What do we learn from pore-spanning membranes? Biochim Biophys Acta - Mol Cell Res 1853:2977–2983 . https://doi.org/10.1016/J.BBAMCR.2015.05.029

131. Möller I, Seeger S (2015) Solid supported lipid bilayers from artificial and natural lipid mixtures – long-term stable, homogeneous and reproducible. J Mater Chem B 3:6046–6056 . https://doi.org/10.1039/C5TB00437C

132. Czajkowsky DM, Sheng S, Shao Z (1998) Staphylococcal α-hemolysin can form hexamers in phospholipid bilayers. J Mol Biol 276:325–330 . https://doi.org/10.1006/JMBI.1997.1535

133. Kakimoto Y, Tero R (2018) Supported Lipid Bilayers of Escherichia coli Extracted Lipids and Their Calcium Dependence. Front Mater 5:48 . https://doi.org/10.3389/fmats.2018.00048

134. Lind TK, Wacklin H, Schiller J, Moulin M, Haertlein M, Pomorski TG, Cárdenas M (2015) Formation and Characterization of Supported Lipid Bilayers Composed of Hydrogenated and Deuterated Escherichia coli Lipids. PLoS One 10:e0144671 . https://doi.org/10.1371/journal.pone.0144671

135. Konarzewska D, Juhaniewicz J, Güzeloğlu A, Sęk S (2017) Characterization of planar biomimetic lipid films composed of phosphatidylethanolamines and phosphatidylglycerols from Escherichia coli. Biochim Biophys Acta - Biomembr 1859:475–483 . https://doi.org/10.1016/J.BBAMEM.2017.01.010

136. Ni T, Jiao F, Yu X, Aden S, Ginger L, Williams SI, Bai F, Pražák V, Karia D, Stansfeld P,

Zhang P, Munson G, Anderluh G, Scheuring S, Gilbert RJC (2020) Structure and mechanism of bactericidal mammalian perforin-2, an ancient agent of innate immunity. Sci Adv 6:eaax8286 . https://doi.org/10.1126/sciadv.aax8286

137. Parsons ES, Stanley GJ, Pyne ALB, Hodel AW, Nievergelt AP, Menny A, Yon AR, Rowley A, Richter RP, Fantner GE, Bubeck D, Hoogenboom BW (2019) Single-molecule kinetics of pore assembly by the membrane attack complex. Nat Commun 10:2066 . https://doi.org/10.1038/s41467-019-10058-7

138. Lee T-H, Heng C, Swann MJ, Gehman JD, Separovic F, Aguilar M-I (2010) Real-time quantitative analysis of lipid disordering by aurein 1.2 during membrane adsorption, destabilisation and lysis. Biochim Biophys Acta - Biomembr 1798:1977–1986 . https://doi.org/10.1016/J.BBAMEM.2010.06.023

139. Soblosky L, Ramamoorthy A, Chen Z (2015) Membrane interaction of antimicrobial peptides using E. coli lipid extract as model bacterial cell membranes and SFG spectroscopy. Chem Phys Lipids 187:20–33 . https://doi.org/10.1016/J.CHEMPHYSLIP.2015.02.003

140. Rakshit T, Senapati S, Parmar VM, Sahu B, Maeda A, Park PS-H (2017) Adaptations in rod outer segment disc membranes in response to environmental lighting conditions. Biochim Biophys acta Mol cell Res 1864:1691–1702 . https://doi.org/10.1016/j.bbamcr.2017.06.013

141. Müller DJ, Schabert FA, Büldt G, Engel A (1995) Imaging purple membranes in aqueous solutions at sub-nanometer resolution by atomic force microscopy. Biophys J 68:1681–1686 . https://doi.org/10.1016/S0006-3495(95)80345-0

142. Kumar S, Cartron ML, Mullin N, Qian P, Leggett GJ, Hunter CN, Hobbs JK (2017) Direct Imaging of Protein Organization in an Intact Bacterial Organelle Using High-Resolution Atomic Force Microscopy. ACS Nano 11:126–133 . https://doi.org/10.1021/acsnano.6b05647

143. Robson A-L, Dastoor PC, Flynn J, Palmer W, Martin A, Smith DW, Woldu A, Hua S (2018) Advantages and Limitations of Current Imaging Techniques for Characterizing Liposome Morphology. Front Pharmacol 9:80 . https://doi.org/10.3389/fphar.2018.00080

144. Heesterbeek DA, Bardoel BW, Parsons ES, Bennett I, Ruyken M, Doorduijn DJ, Gorham RD, Berends ET, Pyne AL, Hoogenboom BW, Rooijakkers SH (2019) Bacterial killing by complement requires membrane attack complex formation via surface-bound C5 convertases. EMBO J 38: . https://doi.org/10.15252/embj.201899852

145. Jin M, Lu F, Belkin MA (2017) High-sensitivity infrared vibrational nanospectroscopy in water. Light Sci Appl 6:e17096 . https://doi.org/10.1038/lsa.2017.96

146. Uchihashi T, Scheuring S (2018) Applications of high-speed atomic force microscopy to real-time visualization of dynamic biomolecular processes. Biochim Biophys Acta - Gen Subj 1862:229–240 . https://doi.org/10.1016/J.BBAGEN.2017.07.010

147. Ruan Y, Miyagi A, Wang X, Chami M, Boudker O, Scheuring S (2017) Direct visualization of glutamate transporter elevator mechanism by high-speed AFM. Proc Natl Acad Sci U S A 114:1584–1588 . https://doi.org/10.1073/pnas.1616413114

148. Salvador-Gallego R, Mund M, Cosentino K, Schneider J, Unsay J, Schraermeyer U, Engelhardt J, Ries J, García-Sáez AJ (2016) Bax assembly into rings and arcs in apoptotic mitochondria is linked to membrane pores. EMBO J 35:389–401 . https://doi.org/10.15252/embj.201593384

149. Yilmaz N, Kobayashi T (2016) Assemblies of pore-forming toxins visualized by atomic force microscopy. Biochim Biophys Acta - Biomembr 1858:500–511 . https://doi.org/10.1016/J.BBAMEM.2015.11.005

150. Mulvihill E, Sborgi L, Mari SA, Pfreundschuh M, Hiller S, Müller DJ (2018) Mechanism of membrane pore formation by human gasdermin-D. EMBO J 37:e98321 . https://doi.org/10.15252/embj.201798321

151. Hodel AW, Leung C, Dudkina N V, Saibil HR, Hoogenboom BW (2016) Atomic force microscopy of membrane pore formation by cholesterol dependent cytolysins. Curr Opin Struct Biol 39:8–15 . https://doi.org/10.1016/j.sbi.2016.03.005

152. Ewald M, Henry S, Lambert E, Feuillie C, Bobo C, Cullin C, Lecomte S, Molinari M (2019) High speed atomic force microscopy to investigate the interactions between toxic Aβ $_{1-42}$ peptides and model membranes in real time: impact of the membrane composition. Nanoscale 11:7229–7238 . https://doi.org/10.1039/C8NR08714H

153. Choi H, Rangarajan N, Weisshaar JC (2016) Lights, Camera, Action! Antimicrobial Peptide Mechanisms Imaged in Space and Time. Trends Microbiol 24:111–122 . https://doi.org/10.1016/j.tim.2015.11.004

154. Zhang X, Wang Y, Liu L, Wei Y, Shang N, Zhang X, Li P (2016) Two-peptide bacteriocin PlnEF causes cell membrane damage to Lactobacillus plantarum. Biochim Biophys Acta - Biomembr 1858:274–280 . https://doi.org/10.1016/J.BBAMEM.2015.11.018

155. Liou J-W, Hung Y-J, Yang C-H, Chen Y-C (2015) The antimicrobial activity of gramicidin A is associated with hydroxyl radical formation. PLoS One 10:e0117065 . https://doi.org/10.1371/journal.pone.0117065

156. Torcato IM, Huang Y-H, Franquelim HG, Gaspar D, Craik DJ, Castanho MARB, Troeira Henriques S (2013) Design and characterization of novel antimicrobial peptides, R-BP100 and RW-BP100, with activity against Gram-negative and Gram-positive bacteria. Biochim Biophys Acta - Biomembr 1828:944–955 . https://doi.org/10.1016/J.BBAMEM.2012.12.002

157. Su H-N, Chen Z-H, Song X-Y, Chen X-L, Shi M, Zhou B-C, Zhao X, Zhang Y-Z (2012) Antimicrobial Peptide Trichokonin VI-Induced Alterations in the Morphological and Nanomechanical Properties of Bacillus subtilis. PLoS One 7:e45818 . https://doi.org/10.1371/journal.pone.0045818

158. Li A, Lee PY, Ho B, Ding JL, Lim CT (2007) Atomic force microscopy study of the antimicrobial action of Sushi peptides on Gram negative bacteria. Biochim Biophys Acta - Biomembr 1768:411–418 . https://doi.org/10.1016/j.bbamem.2006.12.010

159. Zdybicka-Barabas A, Stączek S, Pawlikowska-Pawlęga B, Mak P, Luchowski R, Skrzypiec K, Mendyk E, Wydrych J, Gruszecki WI, Cytryńska M (2019) Studies on the interactions of neutral Galleria mellonella cecropin D with living bacterial cells. Amino Acids 51:175–191 . https://doi.org/10.1007/s00726-018-2641-4

160. Dias SA, Freire JM, Pérez-Peinado C, Domingues MM, Gaspar D, Vale N, Gomes P, Andreu D, Henriques ST, Castanho MARB, Veiga AS (2017) New Potent Membrane-Targeting Antibacterial Peptides from Viral Capsid Proteins. Front Microbiol 8:775 . https://doi.org/10.3389/fmicb.2017.00775

161. Oliveira M, Gomes-Alves AG, Sousa C, Mirta Marani M, Plácido A, Vale N, Delerue-Matos C, Gameiro P, Kückelhaus SAS, Tomas AM, S. A. Leite JR, Eaton P (2016) Ocellatin-PT antimicrobial peptides: High-resolution microscopy studies in antileishmania models and interactions with mimetic membrane systems. Biopolymers 105:873–886 . https://doi.org/10.1002/bip.22925

162. Domingues MM, Silva PM, Franquelim HG, Carvalho FA, Castanho MARB, Santos NC (2014) Antimicrobial protein rBPI21-induced surface changes on Gram-negative and Gram-positive bacteria. Nanomedicine Nanotechnology, Biol Med 10:543–551 . https://doi.org/10.1016/j.nano.2013.11.002

163. Maraming P, Klaynongsruang S, Boonsiri P, Peng S, Daduang S, Leelayuwat C, Pientong C, Chung J, Daduang J (2019) The cationic cell-penetrating KT2 peptide promotes cell membrane defects and apoptosis with autophagy inhibition in human HCT 116 colon cancer cells. J Cell Physiol 234:22116–22129 . https://doi.org/10.1002/jcp.28774

164. Gonçalves S, Silva PM, Felício MR, de Medeiros LN, Kurtenbach E, Santos NC (2017) Psd1

Effects on Candida albicans Planktonic Cells and Biofilms. Front Cell Infect Microbiol 7:249 . https://doi.org/10.3389/fcimb.2017.00249

165. Soliman C, Eastwood S, Truong VK, Ramsland PA, Elbourne A (2019) The membrane effects of melittin on gastric and colorectal cancer. PLoS One 14:e0224028 . https://doi.org/10.1371/journal.pone.0224028

166. Overton K, Greer H, Ferguson MA, Spain EM, Elmore DE, Nunez ME, Volle C (2020) Qualitative and Quantitative Changes to E. coli During Treatment with Magainin 2 Observed in Native Conditions by Atomic Force Microscopy. Langmuir 36:650–659 . https://doi.org/10.1021/acs.langmuir.9b02726

167. Mularski A, Wilksch JJ, Hanssen E, Strugnell RA, Separovic F (2016) Atomic force microscopy of bacteria reveals the mechanobiology of pore forming peptide action. Biochim Biophys Acta - Biomembr 1858:1091–1098 . https://doi.org/10.1016/J.BBAMEM.2016.03.002

168. Mortensen NP, Fowlkes JD, Sullivan CJ, Allison DP, Larsen NB, Molin S, Doktycz MJ (2009) Effects of Colistin on Surface Ultrastructure and Nanomechanics of Pseudomonas aeruginosa Cells. Langmuir 25:3728–3733 . https://doi.org/10.1021/la803898g

169. Mikuláss KR, Nagy K, Bogos B, Szegletes Z, Kovács E, Farkas A, Váró G, Kondorosi É, Kereszt A (2016) Antimicrobial nodule-specific cysteine-rich peptides disturb the integrity of bacterial outer and inner membranes and cause loss of membrane potential. Ann Clin Microbiol Antimicrob 15:43 . https://doi.org/10.1186/s12941-016-0159-8

170. Wang C, Zolotarskaya OY, Nair SS, Ehrhardt CJ, Ohman DE, Wynne KJ, Yadavalli VK (2016) Real-Time Observation of Antimicrobial Polycation Effects on Escherichia coli : Adapting the Carpet Model for Membrane Disruption to Quaternary Copolyoxetanes. Langmuir 32:2975–2984 . https://doi.org/10.1021/acs.langmuir.5b04247

171. Pérez-Peinado C, Dias SA, Domingues MM, Benfield AH, Freire JM, Rádis-Baptista G, Gaspar D, Castanho MARB, Craik DJ, Henriques ST, Veiga AS, Andreu D (2018) Mechanisms of bacterial membrane permeabilization by crotalicidin (Ctn) and its fragment Ctn(15–34), antimicrobial peptides from rattlesnake venom. J Biol Chem 293:1536–1549 . https://doi.org/10.1074/jbc.RA117.000125

172. Nagy K, Mikuláss KR, Végh AG, Kereszt A, Kondorosi É, Váró G, Szegletes Z (2015) Interaction of cysteine-rich cationic antimicrobial peptides with intact bacteria and model membranes. Gen Physiol Biophys 34:135–144 . https://doi.org/10.4149/gpb_2015002

173. Fantner GE, Barbero RJ, Gray DS, Belcher AM (2010) Kinetics of antimicrobial peptide

activity measured on individual bacterial cells using high-speed atomic force microscopy. Nat Nanotechnol 5:280–285 . https://doi.org/10.1038/nnano.2010.29

174. Benn G, Pyne ALB, Ryadnov MG, Hoogenboom BW (2019) Imaging live bacteria at the nanoscale: Comparison of immobilisation strategies. Analyst 144:6944–6952 . https://doi.org/10.1039/c9an01185d

175. Pasquina-Lemonche L, Burns J, Turner RD, Kumar S, Tank R, Mullin N, Wilson JS, Chakrabarti B, Bullough PA, Foster SJ, Hobbs JK (2020) The architecture of the Gram-positive bacterial cell wall. Nature 582:294–297 . https://doi.org/10.1038/s41586-020-2236-6

176. Alsteens D, Dupres V, Yunus S, Latgé J-P, Heinisch JJ, Dufrêne YF (2012) High-Resolution Imaging of Chemical and Biological Sites on Living Cells Using Peak Force Tapping Atomic Force Microscopy. Langmuir 28:16738–16744 . https://doi.org/10.1021/la303891j

177. Formosa C, Schiavone M, Boisrame A, Richard ML, Duval RE, Dague E (2015) Multiparametric imaging of adhesive nanodomains at the surface of Candida albicans by atomic force microscopy. Nanomedicine Nanotechnology, Biol Med 11:57–65 . https://doi.org/10.1016/j.nano.2014.07.008

178. Alsteens D, Müller DJ, Dufrêne YF (2017) Multiparametric Atomic Force Microscopy Imaging of Biomolecular and Cellular Systems. Acc Chem Res 50:924–931 . https://doi.org/10.1021/acs.accounts.6b00638

179. Hayouka Z, Bella A, Stern T, Ray S, Jiang H, Grovenor CRM, Ryadnov MG (2017) Binary Encoding of Random Peptide Sequences for Selective and Differential Antimicrobial Mechanisms. Angew Chemie Int Ed 56:8099–8103 . https://doi.org/10.1002/anie.201702313

180. Odermatt PD, Shivanandan A, Deschout H, Jankele R, Nievergelt AP, Feletti L, Davidson MW, Radenovic A, Fantner GE (2015) High-Resolution Correlative Microscopy: Bridging the Gap between Single Molecule Localization Microscopy and Atomic Force Microscopy. Nano Lett 15:4896–4904 . https://doi.org/10.1021/acs.nanolett.5b00572

181. Xiao L, Schultz ZD (2018) Spectroscopic Imaging at the Nanoscale: Technologies and Recent Applications. Anal Chem 90:440–458 . https://doi.org/10.1021/acs.analchem.7b04151